A&AE 520

EXPERIMENTAL AERODYNAMICS

John Sullivan
Feb. 2004

NOTES

ON

LASER DOPPLER VELOCIMETRY

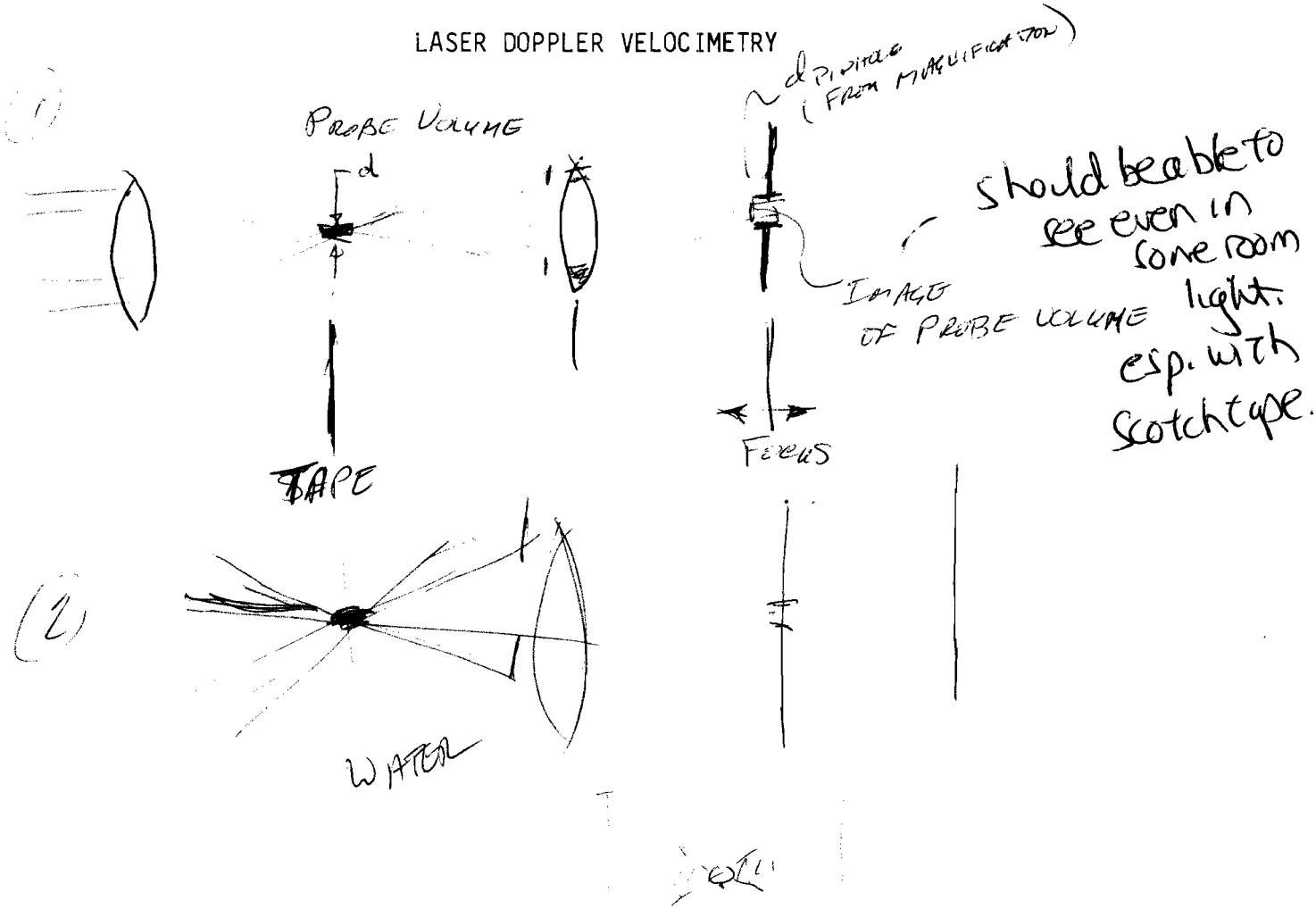

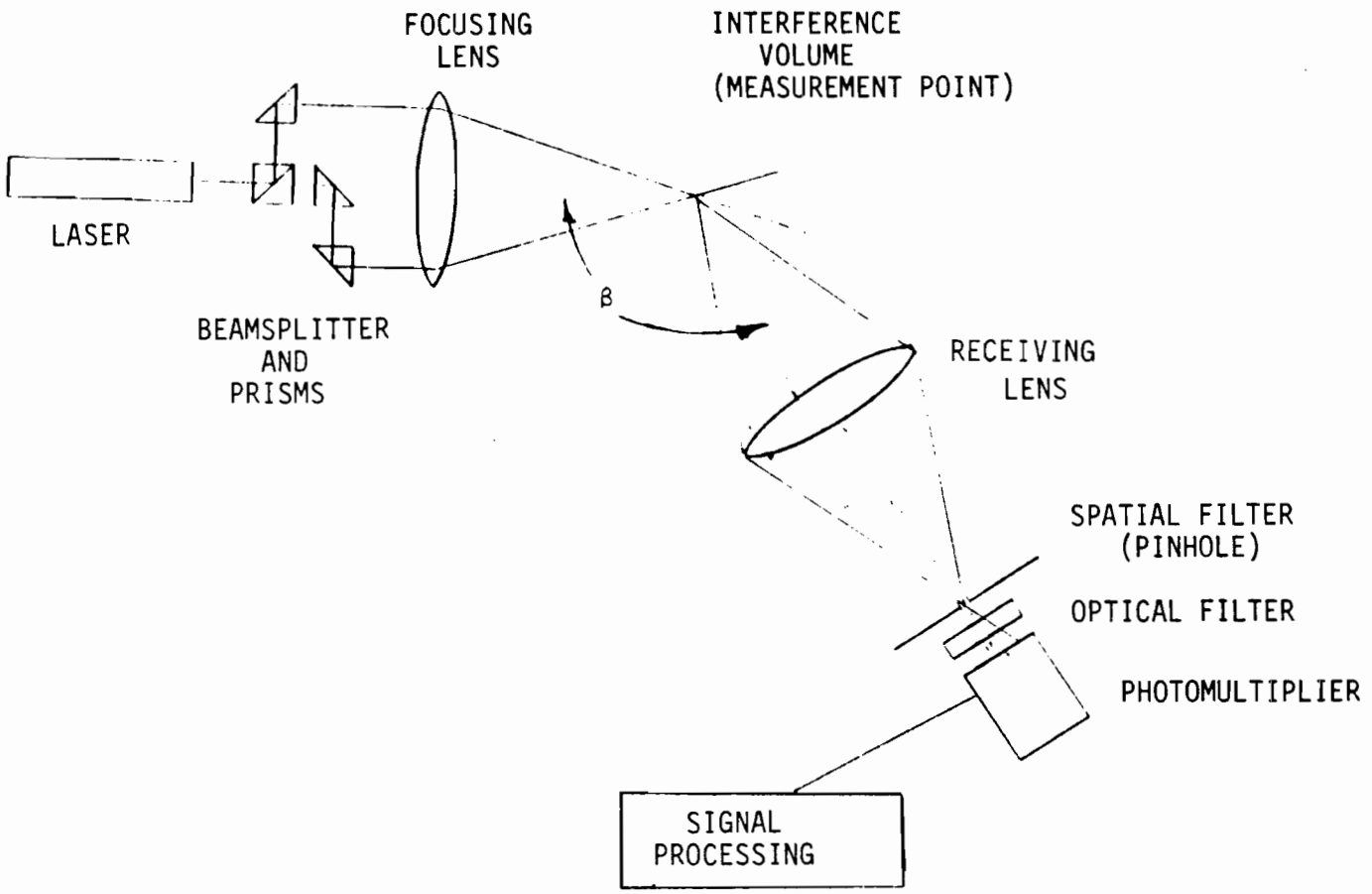

The most common optical arrangement for one dimensional LDV Systems is shown in the Figure. It measures the component of the fluid velocity lying in the plane of the paper and perpendicular to the bisector of the angle between the two transmitted beams. When the angle between the transmitting optics and the receiving optics, β, is equal to 180° the LDV system is called a "forward scatter system." When β=0 it is called a "backscatter system."

The components of the LDV system are:

TRANSMISSION OPTICS

- LASER
- BEAMSPLITTER
- PRISMS & MIRRORS
- WAVEPLATES
- LENS

RECEIVING OPTICS

- LENS
- COLOR FILTER
- SPATIAL FILTER (PINHOLE)
- PHOTO MULTIPLIER

THE LASER DOPPLER VELOCIMETER

2.1. Introduction

The principle of operation of two types of laser Doppler velocimeters will be considered in this chapter. A detailed description of the scattering process, operation, construction, and associated electronics for one of these--the dual scatter system-- will also be given.

2.2. Basic Principles of Laser Doppler Velocimetry

Since the introduction of the laser Doppler velocimeter (LDV) in 1964 by Yeh and Cummings (Ref 1) numerous systems have been reported. Two of these, the cross beam-reference beam system (Fig. 1a) of ref. 2, and the dual scatter system (Fig. 1b) of refs 3 and 37 will be considered. These two were chosen because they are self aligning; that is, once the beams are made to intersect at the probing point and pass through the aperture in front of the photomultiplier tube, the system is aligned. This eliminates the tedious alignment and vibration problems of other systems.

Laser light that is scattered from particles (smoke, dirt, polystyrene spheres) moving at the local fluid velocity undergoes a Doppler shift given by

$$f = f_o + \frac{\vec{V}\cdot(\hat{k}_s - \hat{k}_i)}{\lambda} + O\left(\frac{|\vec{V}|}{c}\right) \qquad (1)$$

where

f_o, λ, $\hat{k}_I$ = frequency, wavelength and unit vector in the propagation direction of the incident laser beam

$\vec{V}$ = velocity of particle

$\hat{k}_s$ = unit vector in the direction that the scattered light is detected

c = velocity of light

The frequency of the scattered radiation f, which is of the order of light frequencies ($\sim 5 \times 10^{14}$ cy/sec) can be detected either directly using a Fabry-Perot interferometer or can be heterodyned with some light wave at a known frequency to obtain a signal whose frequency is equal to the shift of the laser light frequency. The present resolution of Fabry-Perot interferometers is only $\sim$2MHz which implies a velocity resolution of $\sim$10 ft/sec. For the present study this is inadequate so a heterodyning system is used.

In the two types of heterodyne systems studied the cross-beam reference beam system (Fig. 1a) heterodynes the scattered radiation with radiation at the laser frequency f_o and the dual scatter system (Fig. 1b) heterodynes the scattered radiation of two different incident beams. In both cases the difference frequency is calculated, using Eq. 1 and the geometry of Fig. 1, to be

$$f_D = \frac{2u}{\lambda} \sin\frac{\theta}{2}$$

where U is the velocity component in a direction perpendicular to the bisector of the angle between two beams. Fig. 2 shows f_D versus U for various values of θ with λ=6328Å, the wavelength of a He Ne laser. It should be noted that there is a 180° amgiguity in determining direction of U. The plus or minus direction of U must be determined by prior knowledge or flow visualization.

The output signal of the photomultiplier (P.M.) tube is proportional to the intensity which for the reference beam system is

$$I_{RB} = (\vec{E}_R + \vec{E}_s)\cdot(\vec{E}_R + \vec{E}_s)^*$$

$$I_{RB} = |\vec{E}_R|^2 + |\vec{E}_s(t)|^2 + 2\vec{E}_R\cdot\vec{E}_s(t)\cos(2\pi f_D t)$$

$\vec{E}_R$ = electric field of reference beam

$\vec{E}_S$ = scattered electric field

when a single particle traverses the measuring volume. This produces an output like that shown in Fig. 3a. The d.c. level is essentially constant since $E_s(t) << E_c$. The a.c. component is modulated by the term, $E_R E_s(t)$ which is generally a gaussian.

In the dual scatter system the light scattered from one beam is heterodyned with light scattered from the other beam resulting in

$$I_{DS} = |\vec{E}_{s_1}(t)|^2 + |\vec{E}_{s_2}(t)|^2 + 2\,\vec{E}_{s_1}(t)\cdot\vec{E}_{s_2}(t)\cos(2\pi f_D t)$$

$\vec{E}_{s_1}$ = electric field scattered by beam one

$\vec{E}_{s_2}$ = electric field scattered by beam two

The results for $E_{s_1}(t) = E_{s_2}(t)$ are shown in Fig. 3b. The d.c. component is now replaced by a low frequency component. The actual signal when a .0002 wire traverses the measuring volume is shown in the oscilloscope trace of Fig. 4a. When the wire doesn't pass

through the center of the measuring volume a signal (Fig. 4b) containing a large amount of the low frequency component and small amount of the Doppler signal component is obtained.

In the present investigation more than one scatterer will be in the measuring volume at one time resulting in a signal which is the sum of the signals from individual particles. A typical "continuous" signal for a dual scatter system is shown in Fig. 4c. This signal was obtained from a rotating ground glass disk. It shows the general features of dual scattering; namely, a low frequency component and low frequency modulation of the Doppler signal. The low frequency modulation is a result of random constructive and destructive interference among the waves scattered by many particles, causing the signal to go randomly to zero during severe destructive interference. This phenomenon, called "drop-out", and the low frequency component, are the major problems in the electronic processing of the signal.

A comparison of the frequency spectrums of the two systems is shown in Fig. 5 for scattering from a ground glass disk and a turbulent jet. Although the magnitudes of the signals are about equal, the low frequency components in the dual scatter system are greater.

The object of this investigation is to determine which of the two systems will give a better signal-to-noise ratio. The reference beam system has the advantage that the signal can be increased by increasing the strength of the reference beam. However, the solid angle through which scattered light may be collected is limited since the Doppler shift $\frac{\vec{V}}{\lambda}\cdot(\hat{k}_s - \hat{k}_I)$

is a function of viewing direction $\hat{k}_s$ so that at large solid angles the Doppler frequency would be unacceptably broadened. On the other hand, the frequency $\frac{\vec{v}}{\lambda}\cdot(\hat{k}_{I_1}-\hat{k}_{I_2})$ of a dual scatter system depends only on the incident beam directions $\hat{k}_{I_1}, \hat{k}_{I_2}$ so that the solid angle for viewing scattered radiation is unlimited. However, the strength of the signal from a dual scatter system is determined entirely by the scattering process. Also there will be more low frequency components in the dual scatter system.

This initial investigation did not indicate that one system was clearly superior but that both performed adequately. At this point it was felt that further comparison would not be fruitful, and the dual scatter system was chosen for further study.

2.3. Scattering By a Spherical Particle

The far field solution for the electric field of an incident plane wave traveling in the z-direction and linearly polarized in the x-direction

$$\vec{E} = \hat{e}_x E_o e^{i(\omega t - kz)}$$ = incident electric field

scattered by a dielectric sphere, of diameter d, located at the origin of the coordinate system (Fig. 6) is given by the Mie solution (Ref. 38).

$$\vec{E}_s = \frac{i E_o e^{i(\omega t - kr)}}{kr}\left[-\sin\phi\, S_1(\theta,\alpha,n)\,\hat{e}_\phi + \cos\phi\, S_{11}(\theta,\alpha,n)\,\hat{e}_\theta\right]$$

The complex scattering amplitude $S_\perp$ is the scattered component whose electric vector is perpendicular to the plane of observation (the plane determined by the direction of observation and the direction of propagation of the incident beam) and $S_{\parallel}$ the component parallel to the plane of observation. The amplitudes $S_\perp$ and $S_{\parallel}$ are functions of the azimuthal angle θ, the size parameter α

$$\alpha = \frac{kd}{2} = \frac{\pi d}{\lambda}$$

and the index of refraction of the sphere, n. The solution $\vec{E}_s$ is a spherical wave whose polarization depends on the relative amplitudes and phases of the $\hat{e}_\phi$ and $\hat{e}_\theta$ components.

The intensity of the scattered radiation is

$$I = \vec{E}_s \cdot \vec{E}_s^*$$

$$I = \frac{\lambda^2 I_0}{4\pi^2 r^2}\left[i_\perp \sin^2\phi + i_{\parallel} \cos^2\phi \right]$$

where $i_\perp = |S_\perp|^2 \qquad i_{\parallel} = |S_{\parallel}|^2$

The real and imaginary parts of $S_\perp$ and $S_{\parallel}$ are shown in Fig. 7 and $i_\perp$ and $i_{\parallel}$ are shown in Fig. 8. Note that for small θ the values of $i_\perp$ and $i_{\parallel}$ are approximately equal and also that there is no phase shift between them (i.e., $\frac{Im(S_\perp)}{Re(S_\perp)} \simeq \frac{Im(S_{\parallel})}{Re(S_{\parallel})}$). This implies that the scattered radiation is linearly polarized.

For small values of θ the complex amplitudes $S_\perp$ and $S_{\parallel}$ are equal so

$$\vec{E}_s = \frac{i E_0 e^{i(\omega t - kr)}}{kr} S_\perp \left[-\sin\phi\, \hat{e}_\phi + \cos\phi\, \hat{e}_\phi \right]$$

If a lens of focal length f is aligned on the z-axis the scattered radiation is transformed to a plane wave

$$\vec{E}_s = \frac{i E_0 e^{i(\omega t - kz)}}{k f} S_1 \hat{e}_x$$

The polarization of this wave is the same as the incident polarization, a fact that will be used later for separating the components of the velocity vector. Note that this is only valid for small θ, and that the polarization for large θ will not in general be the same as the incident wave.

In the actual LDV system, the laser beam is focused by a lens of focal length f. The electric field in the focal region is given by the plane wave (Ref 46)

$$\vec{E} = \hat{e}_x e^{i(\omega t - kz)} (I_0)^{1/2} e^{-\frac{1}{b_0^2}(x^2 + y^2)}$$

$b_0 = \frac{2F\lambda}{\pi}$ radius of focused spot to $\frac{1}{e^2}$ intensity points

where $F = \frac{f}{2b} = \frac{\text{Focal length}}{\text{Diameter of unfocused laser beam}(1/e^2 \text{ intensity})}$

and I_0 is the total integrated intensity. The power of the laser is related to I_0 by

$$I_0 = \frac{2P_L}{\pi b^2}$$

which was obtained by integrating $\vec{E} \cdot \vec{E}^*$ over the x-y plane.

Although the magnitude of the electric field varies over the particle, this effect will be small since the laser spot size will be $\sim$100 times the diameter of the particle. The electric

field scattered by a particle in the vicinity of a focused laser will be

$$\vec{E}_s = \frac{i\,(I_0)^{1/2}}{kr}\, e^{i(\omega t - kr)}\; e^{-\frac{1}{b_0^2}(x_p^2 + y_p^2)} \times$$

$$\left[-\sin\phi\; S_\perp(\theta,\alpha,n)\,\hat{e}_\phi + \cos\phi\; S_{11}(\theta,\alpha,n)\,\hat{e}_\theta\right]$$

For future use the scattered field from a particle located at an arbitrary point $\vec{r}_p$ by a plane wave with vector $\vec{k}_i$ (lying in z,y plane) is found to be

$$\vec{E}_s = \frac{i(I_0)^{1/2}}{k|r_i|}\, e^{i\left[(\omega t - k|\vec{r}_i| - \vec{k}_i\cdot\vec{r}_p\right]}\; e^{-\frac{1}{b_0^2}(x_{p_i}^2 + y_{p_i}^2)}$$

$$\left[-\sin\phi_i\; S_\perp(\theta_i,\alpha,n)\,\hat{e}_{\phi_i} + \cos\phi_i\; S_{11}(\theta_i,\alpha,n)\,\hat{e}_{\theta_i}\right]$$

where the subscripted coordinates refer to the coordinate system shown in Fig. 9. Since $|\vec{R}| >> |\vec{r}_p|$ the origin of this coordinate system (x_i, y_i, z_i) can be taken at the origin of (x,y,z) so that z_i lies along $\hat{k}_i$ and y_i is in the z,y plane. Also

$$k|r_i| = k|R - r_p| \cong k\left(|\vec{R}| - \frac{\vec{R}}{R}\cdot\vec{r}_p\right) \equiv kR - \vec{k}_s\cdot\vec{r}_p$$

So the scattered field is approximately

$$\vec{E}_s = \frac{i(I_{oi})^{1/2}}{RR} e^{i[(\omega t - (\vec{k}_i - \vec{k}_s)\cdot\vec{r}_p) - kR]} \; e^{-\frac{1}{b^2}(x_{pi}^2 + y_{pi}^2)}$$

$$[-\sin\phi_i \, S_\perp(\theta_i, \alpha, n)\hat{e}_{\phi_i} + \cos\phi_i \, S_{11}(\theta_i, \alpha, n)\hat{e}_{\theta_i}]$$

(2)

2.4. Detailed Description of Dual Scatter System

In the dual scatter system, two parallel laser beams are focused at a common measuring point as shown in Fig. 10. The radiation scattered by beam No. 1 is given by Eq. 2 with i = 1 and that scattered by beam No. 2 is also given by Eq. 2 with i = 2. The subscripted coordinates (x_i, y_i, z_i) or (r_i, θ_i, ϕ_i) refer to coordinates whose z_i axis lies along $\vec{k}_i$ with both $\vec{k}_i$ and y_i in the z,y plane. Since the scattering is linear the electric field at any distant point is just the sum of the two scattered waves. The intensity of light, I, scattered by the two beams at any point on a sphere of radius R is given by

$$I = (\vec{E}_{s_1} + \vec{E}_{s_2}) \cdot (\vec{E}_{s_1} + \vec{E}_{s_2})^*$$

$$I = \frac{\lambda^2}{4\pi^2 r^2} e^{-\frac{2}{b^2}(x_p^2 + y_p^2 \cos^2\frac{\theta_0}{2} + z_p \sin^2\frac{\theta_0}{2})} \times$$

$$\left[\sigma_1 + \sigma_2 + 2\sigma_{12}\cos\left(\frac{2\sin\frac{\theta_0}{2}}{\lambda} y_p\right)\right] \qquad (3)$$

where

$$\sigma_1 = I_{o_1} e^{-\frac{2}{b_o^2}\left[\frac{y_p z_p}{2} \sin\theta_o\right]} \times$$

$$\left[\sin^2\phi_1\, i_\perp(\theta_1) + \cos^2\phi_1\, i_{11}(\theta_1)\right]$$

$$\sigma_2 = I_{o_2} e^{+\frac{2}{b_o^2}\left[\frac{y_p z_p}{2} \sin\theta_o\right]} \times$$

$$\left[\sin^2\phi_2\, i_\perp(\theta_2) + \cos^2\phi_2\, i_{11}(\theta_2)\right]$$

$$\sigma_{12} = (I_{o_1} I_{o_2})^{1/2} \left[\sin\phi_1 \sin\phi_2 \left(i_\perp(\theta_1) i_\perp(\theta_2)\right)^{1/2} \hat{e}_{\phi_1}\cdot\hat{e}_{\phi_2}\right.$$

$$+ \cos\phi_1 \cos\phi_2 \left(i_{11}(\theta_1) i_{11}(\theta_2)\right)^{1/2} \hat{e}_{\theta_1}\cdot\hat{e}_{\theta_2}$$

$$+ \sin\phi_1 \cos\phi_2 \left(i_\perp(\theta_1) i_{11}(\theta_2)\right)^{1/2} \hat{e}_{\theta_1}\cdot\hat{e}_{\phi_2}$$

$$\left. + \cos\phi_1 \sin\phi_2 \left(i_\perp(\theta_2) i_{11}(\theta_1)\right)^{1/2} \hat{e}_{\theta_2}\cdot\hat{e}_{\phi_1}\right]$$

Several conclusions can be drawn from Eq. (3). Setting $\vec{r}_p = \vec{r}_{o_p} + \vec{v}t =$

$(x_{o_p} + ut,\ y_{o_p} + vt,\ z_{o_p} + wt)$

(valid to $\frac{|\vec{v}|}{c}$) the a.c. component has a frequency

$$f_D = \frac{2 \sin\frac{\theta_o}{2}\,|v|}{\lambda}$$

i.e., by measuring this frequency and θ_B the component of velocity in the plane of the two beams and in a direction perpendicular to the bisector of two beams can be determined. The exponent indicates that when a particle is on the ellipsoid

$$\left(\frac{x_p}{b_o}\right)^2 + \left(\frac{y_p}{b_o/\cos\theta_{B/2}}\right)^2 + \left(\frac{z_p}{b_o/\sin\frac{\theta_B}{2}}\right)^2 = 1$$

the intensity will be $1/e^2$ of the intensity for a particle located at (0,0,0). This ellipsoid is called the probe volume. Although the probe volume is actually determined by the minimum detectable signal the $1/e^2$ points provide a good estimate. The volume of the probe is

$$V = \frac{8\pi b_o^3}{3\sin\theta_B}$$

For small values of θ_B, the probe is approximately a cylinder with radius b_o and length $2b_o/\sin(\theta_B/2)$.

The signal from a single particle given by Eq. 3 is the sum of two gaussian pulses and the Doppler shift term with the resulting signal discussed earlier and shown in Fig. 4a. The length of the Doppler pulse is controlled by a gaussian envelope

$$e^{-\frac{2}{b_o^2}\left[(x_{o_p}+ut)^2 + (y_{o_p}+vt)^2\cos^2\frac{\theta_B}{2} + (z_{o_p}+wt)^2\sin^2\frac{\theta_B}{2}\right]}$$

The wider this gaussian envelope the less broad will be the signal in the frequency domain. The best case occurs for $V = W = 0$ $x_{o_f} = y_{o_p} = z_{o_p} = 0$ giving a width

$$\frac{\Delta f}{f} = \frac{1}{2F}\cot\theta_{B/2}$$

It should be noted that this is the minimum broadening that can be expected. Any particle with a V and/or W component and/or not passing directly through the center of the scattering volume ($x_{o_p} \neq 0$, $y_{o_p} \neq 0$, $z_{o_p} \neq 0$) will cause additional broadening.

A useful approximation, and one that is often valid in practice, is to assume $\theta_B \ll 1$ (or $(\pi - \theta_B) \ll 1$) and the solid angle (Ω) over which scattered radiation is collected is also small. Then

$$\phi_1 \cong \phi_2 \cong \phi$$
$$\theta_1 \cong \theta_2 \cong \theta$$
$$i_\perp(\theta_1) \cong i_\perp(\theta_2) \cong i_\perp(\theta)$$
$$i_{11}(\theta_1) \cong i_{11}(\theta_2) = i_{11}(\theta)$$

Also letting $I_{o_i} = I_{o_i} = I_o$ which is the optimum case.

$$I = 2 I_o \left[\sin^2\phi \; i_\perp(\theta) + \cos^2\phi \; i_{11}(\theta) \right] \left\{ e^{-\frac{2}{b_o^2}\left(x_p^2 + y_p^2 \cos^2\frac{\theta_B}{2} + z_p^2 \sin^2\frac{\theta_B}{2}\right.} \right.$$

$$\left. \times \left[\cosh\left(\frac{y_p z_p \sin\frac{\theta_B}{2}}{b_o^2} \right) + \cos 2\pi \left(\frac{2 \sin\frac{\theta_B}{2} y_p}{\lambda} \right) \right] \right\}$$

The term in braces is simply the intensity distribution in the probe volume. This intensity distribution oscillates from $4I_o$ to 0 thus giving rise to a set of interference fringes. The fringe model, first suggested by Rudd, implies that as a particle moves into a bright fringe, it scatters light, then it moves into a dark fringe, then back into a bright fringe

scattering light, etc. Note that this model is only valid for small forward or backward scattering.

Until this point, the polarization of the incident beams has been in the x-direction, i.e., perpendicular to the plane of the two beams. For the small angle scattering case this maximizes the Doppler shift term of the intensity since the fringe contrast will be maximum. To show this consider the a.c. part of the intensity within the probe volume formed by two incident beams with arbitrary linear polarization

$$\vec{E}_{I_1} = E_{a_1}\hat{a}_1 + E_{b_1}\hat{b}_1$$

$$\vec{E}_{I_2} = E_{a_2}\hat{a}_2 + E_{b_2}\hat{b}_2$$

where the unit vectors $\hat{a}$, $\hat{b}$ are shown in Section AA of Fig. 1.

The a.c. or Doppler shift term is

$$\vec{E}_{I_1} \cdot \vec{E}_{I_2} = \left[-E_{a_1}E_{a_2}\cos\theta_B + E_{b_1}E_{b_2} \right] \qquad (4)$$

For arbitrary polarization this equation shows that the signal decreases as θ_B increases. If incident beams are polarized in the $\hat{b}_1$ and $\hat{b}_2$ directions (i.e. $E_{a_1} = E_{a_2} = 0$) then the maximum signal will be obtained. In cases where the scattering is not limited to small angles the polarization of the scattered waves (i.e. $S_\perp$ and $S_{||}$) must be considered.

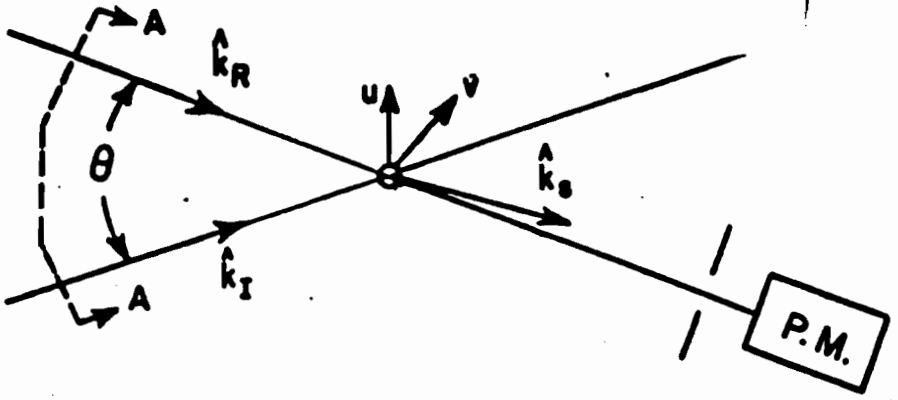

REFERENCE BEAM SYSTEM

Fig. 1a

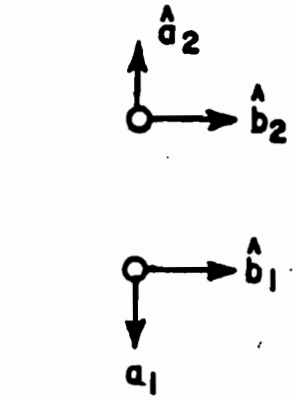

SECTION A-A

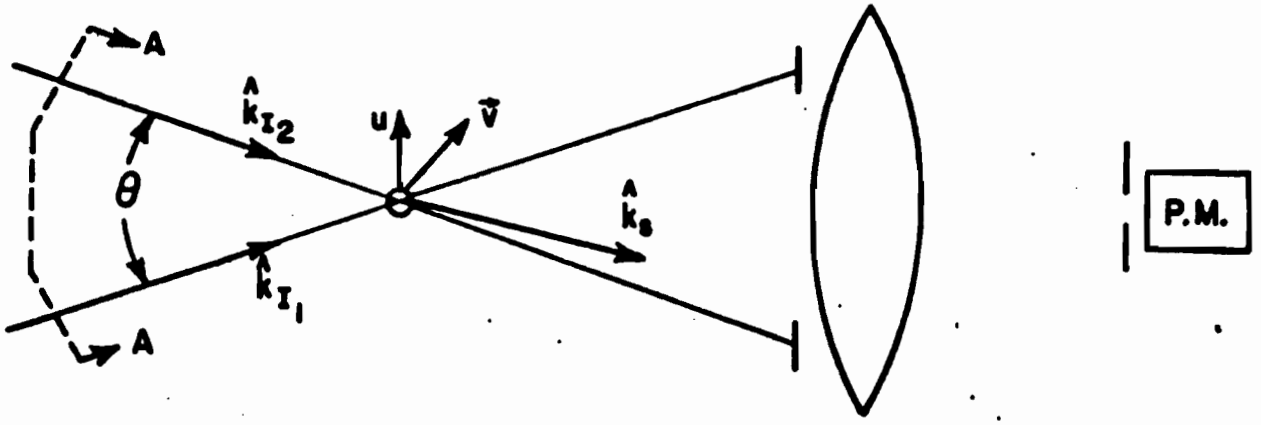

DUAL SCATTER SYSTEM

Fig. 1b

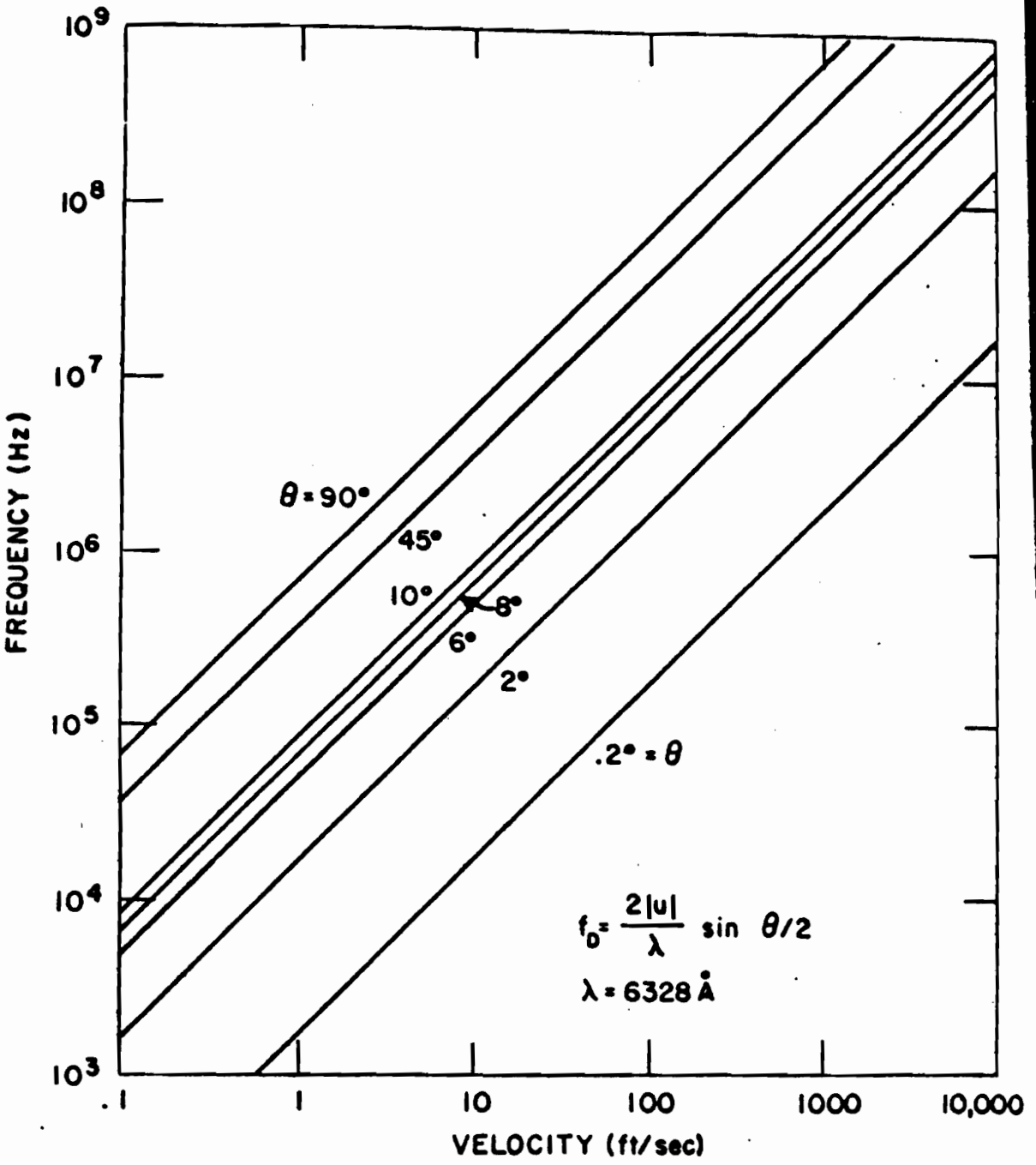

Fig. 2. Doppler shift vs. velocity for He-Ne laser at various scattering angles.

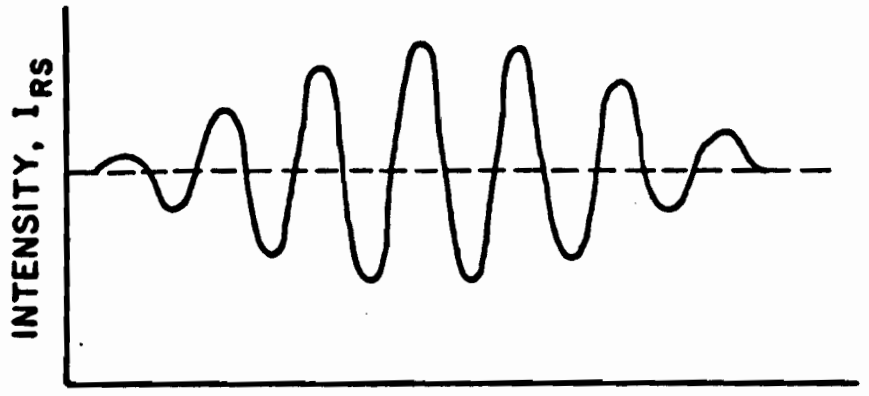

REFERENCE BEAM SYSTEM

Fig. 3a

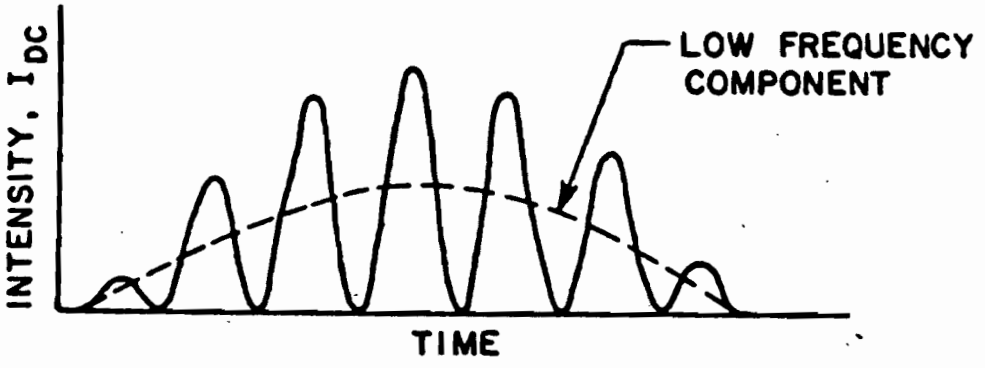

DUAL SCATTER SYSTEM

Fig. 3b

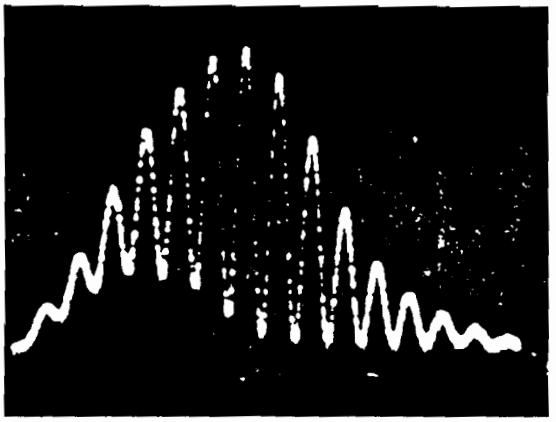

Fig. 4a. Doppler signal from .0002 dia. wire passing through center of probe volume.
Vert.scale 100MV/cm
Horiz. " .1MS/cm

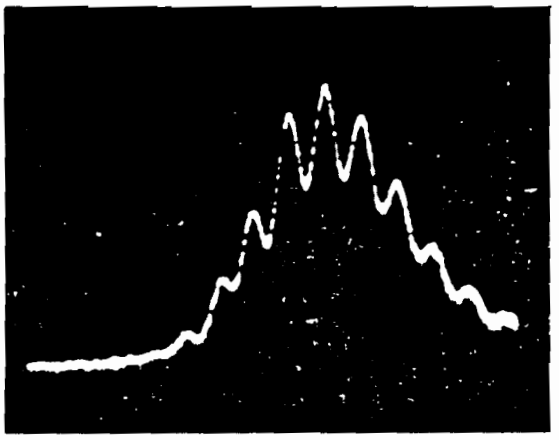

Fig. 4b. Doppler signal from .0002 dia. wire which did not pass through center of probe vol. Scale same as 4a.

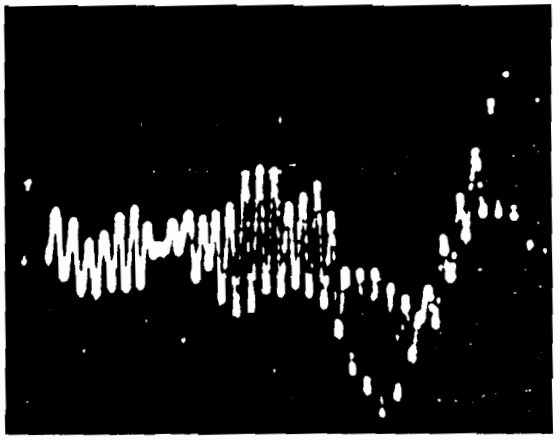

Fig. 4c. Doppler signal from spinning disk.
Vert.scale 100MV cm
Horiz. " .05MS/cm

REFERENCE BEAM

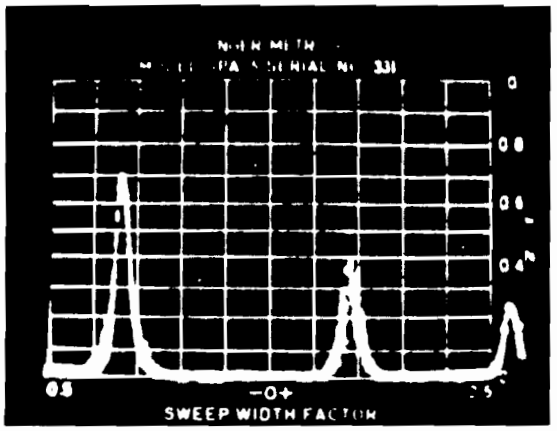

0 500KHZ

1. Disk

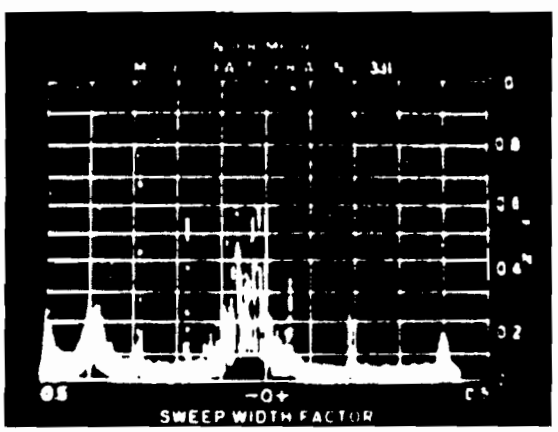

0 1MHZ 2MHZ

2. Smoke Jet

DUAL SCATTER

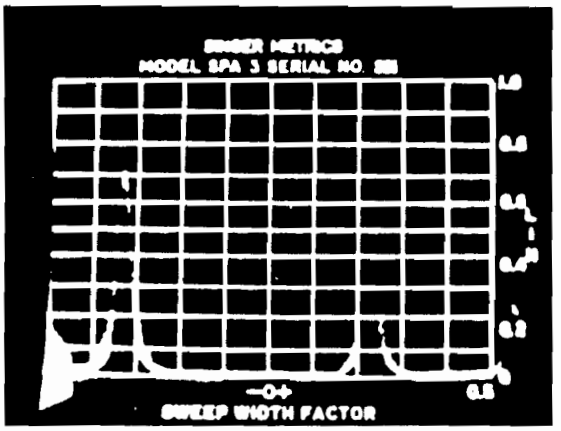

0 500KHZ

1. Disk

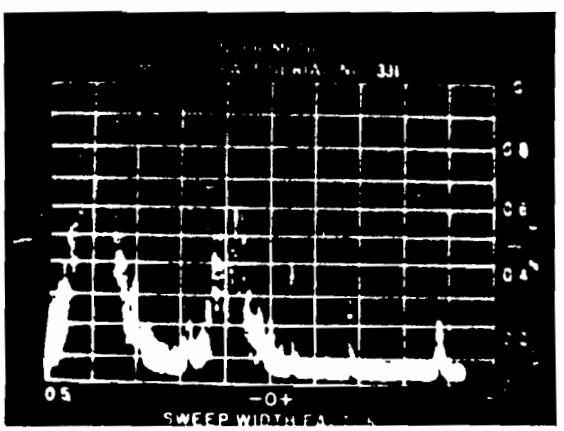

0 1MHZ 2 MHZ

2. Smoke Jet

Fig. 5. Signals from Ref. Beam & Dual Scatter Systems

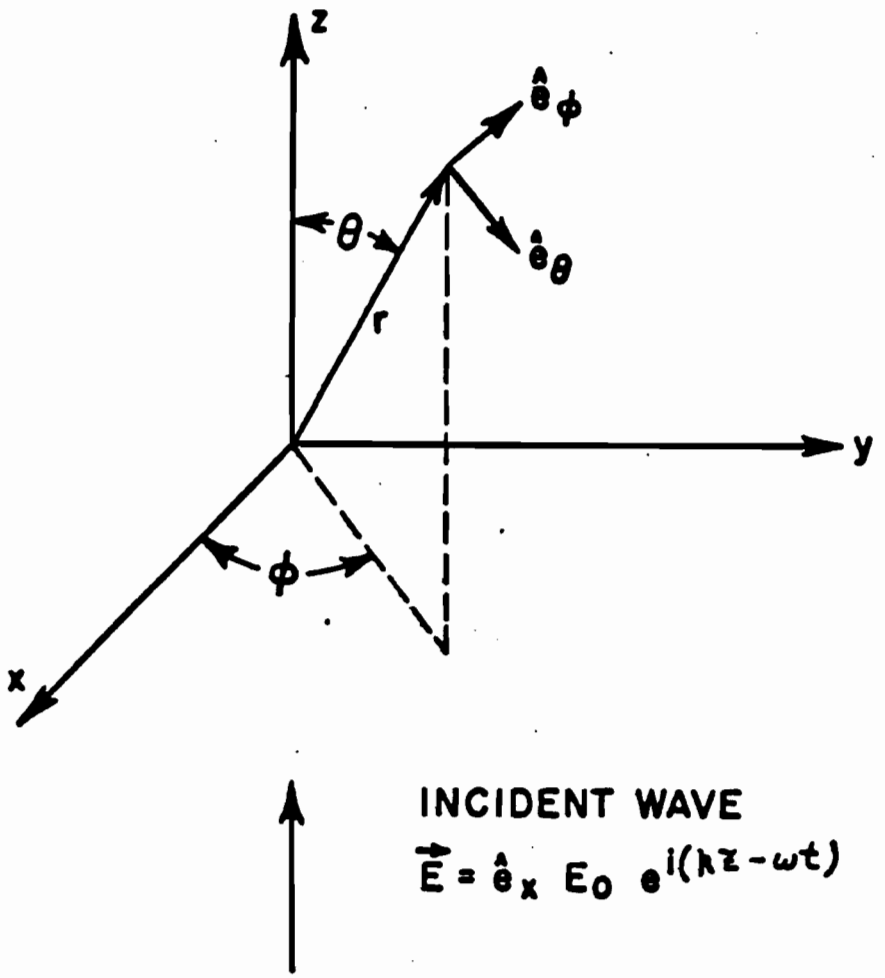

Fig. 6. Coordinate System for Mie Scattering

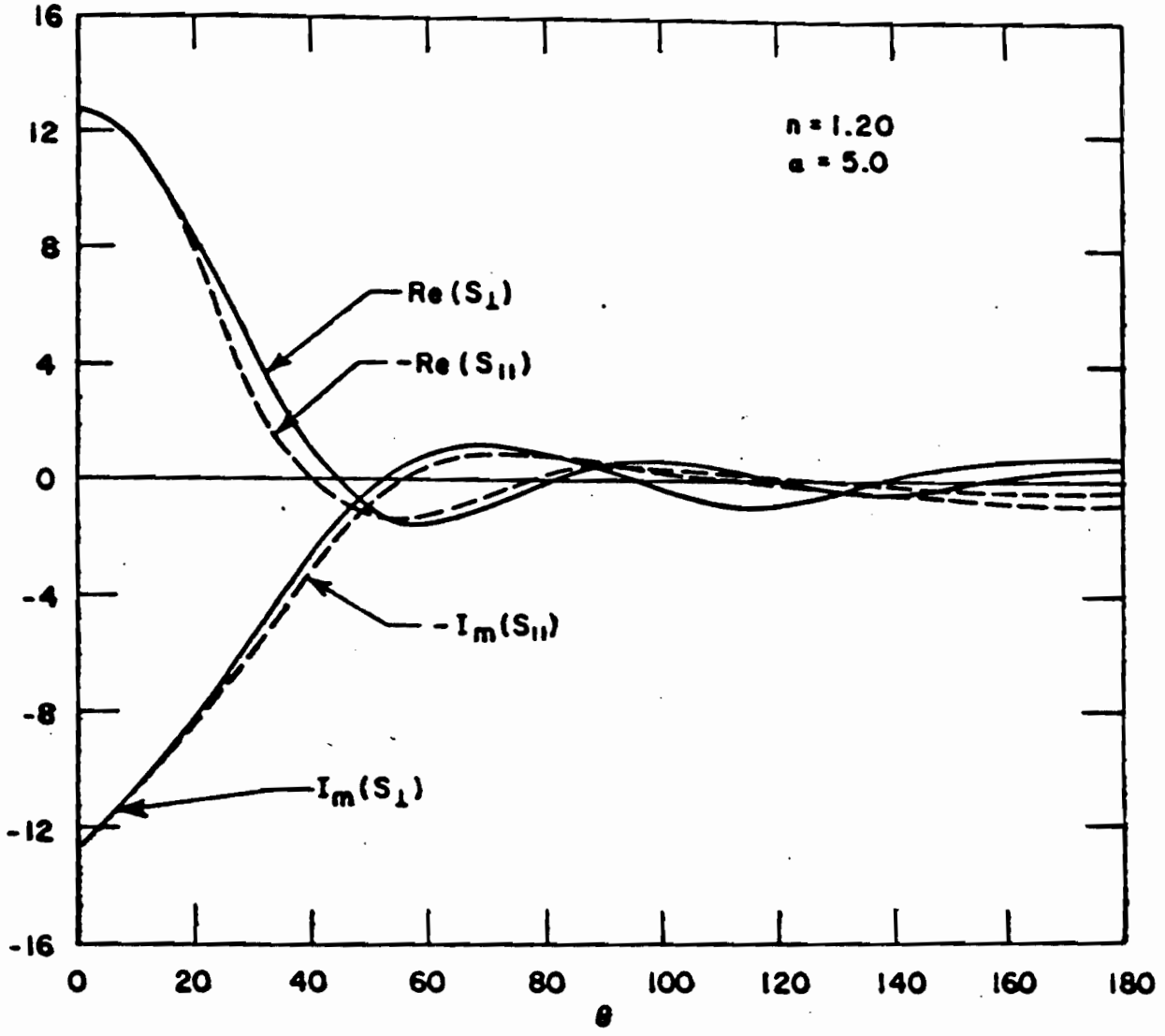

Fig. 7. Real and Imaginary Parts of S

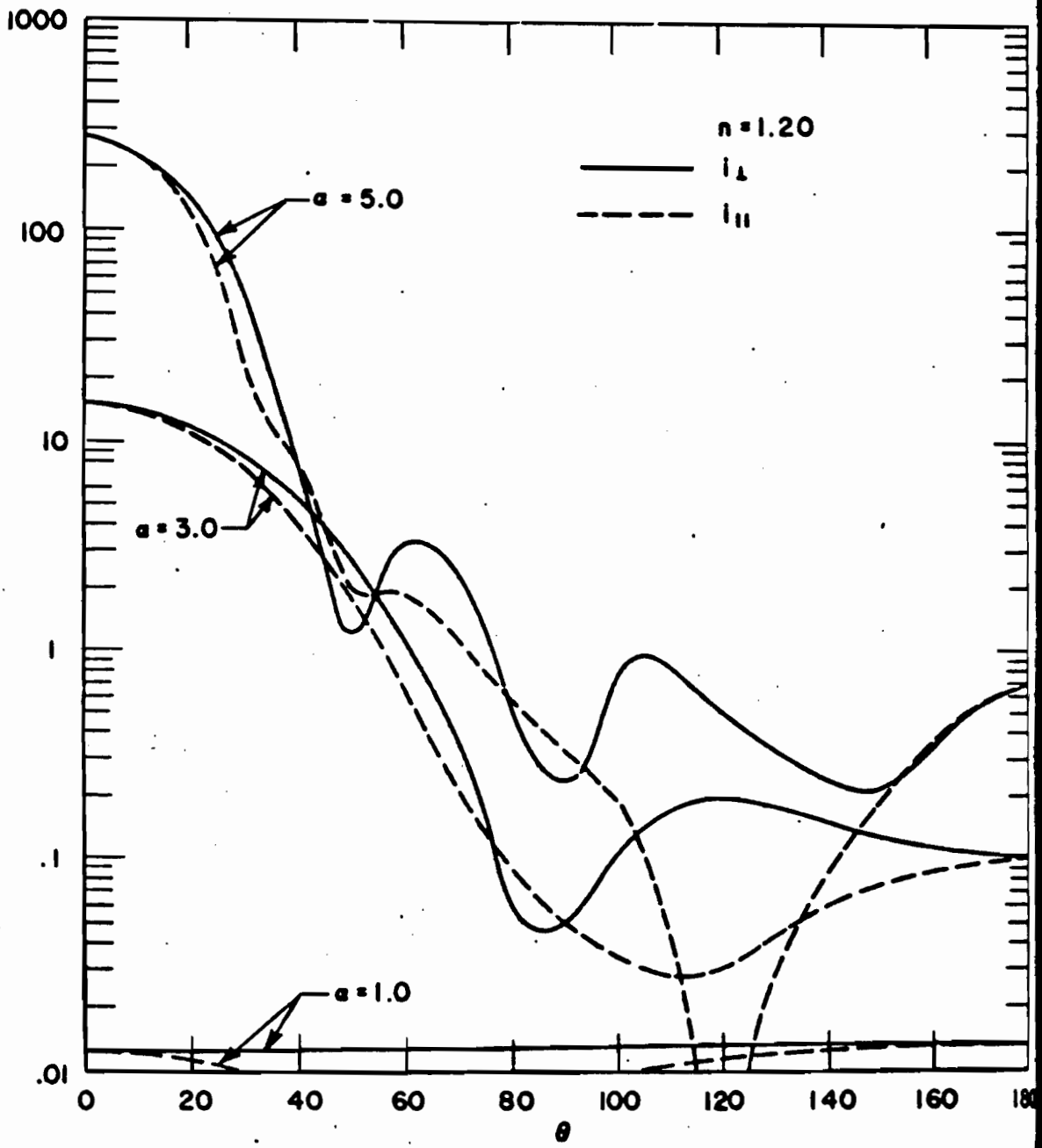

Fig. 8. Scattering Intensity Functions

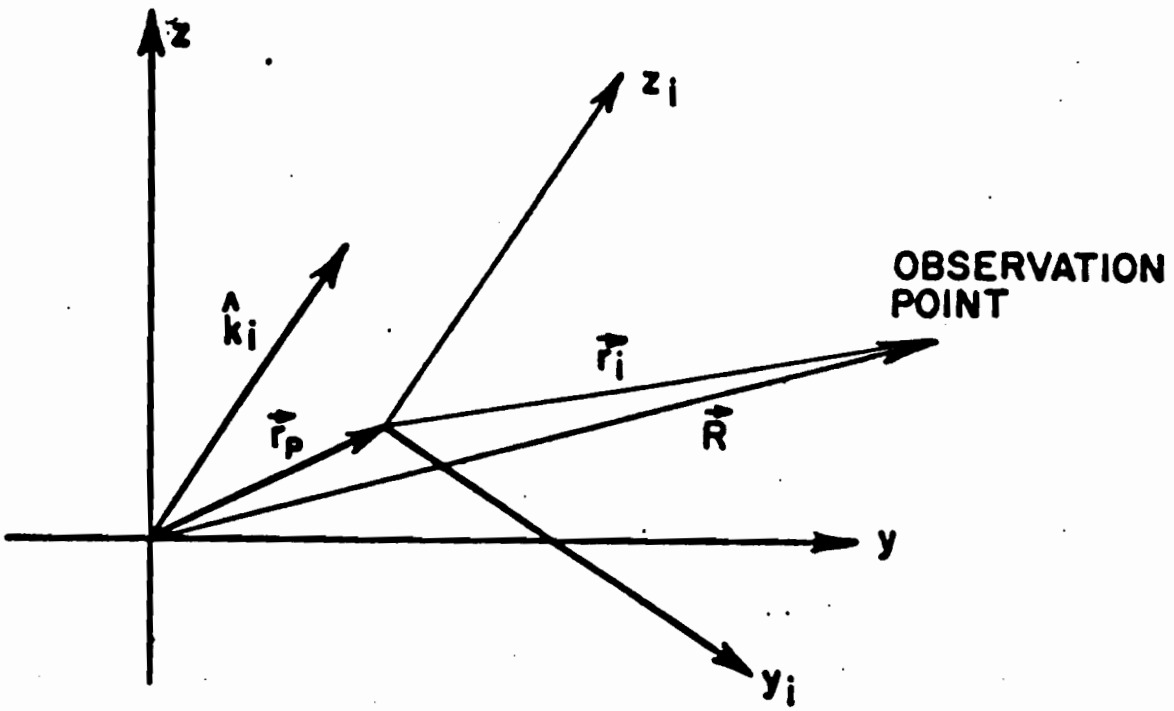

Fig. 9. Coordinate System for Scattering of Incident Wave in $\hat{k}_i$ Direction by Particle Located at $\vec{r}_p$

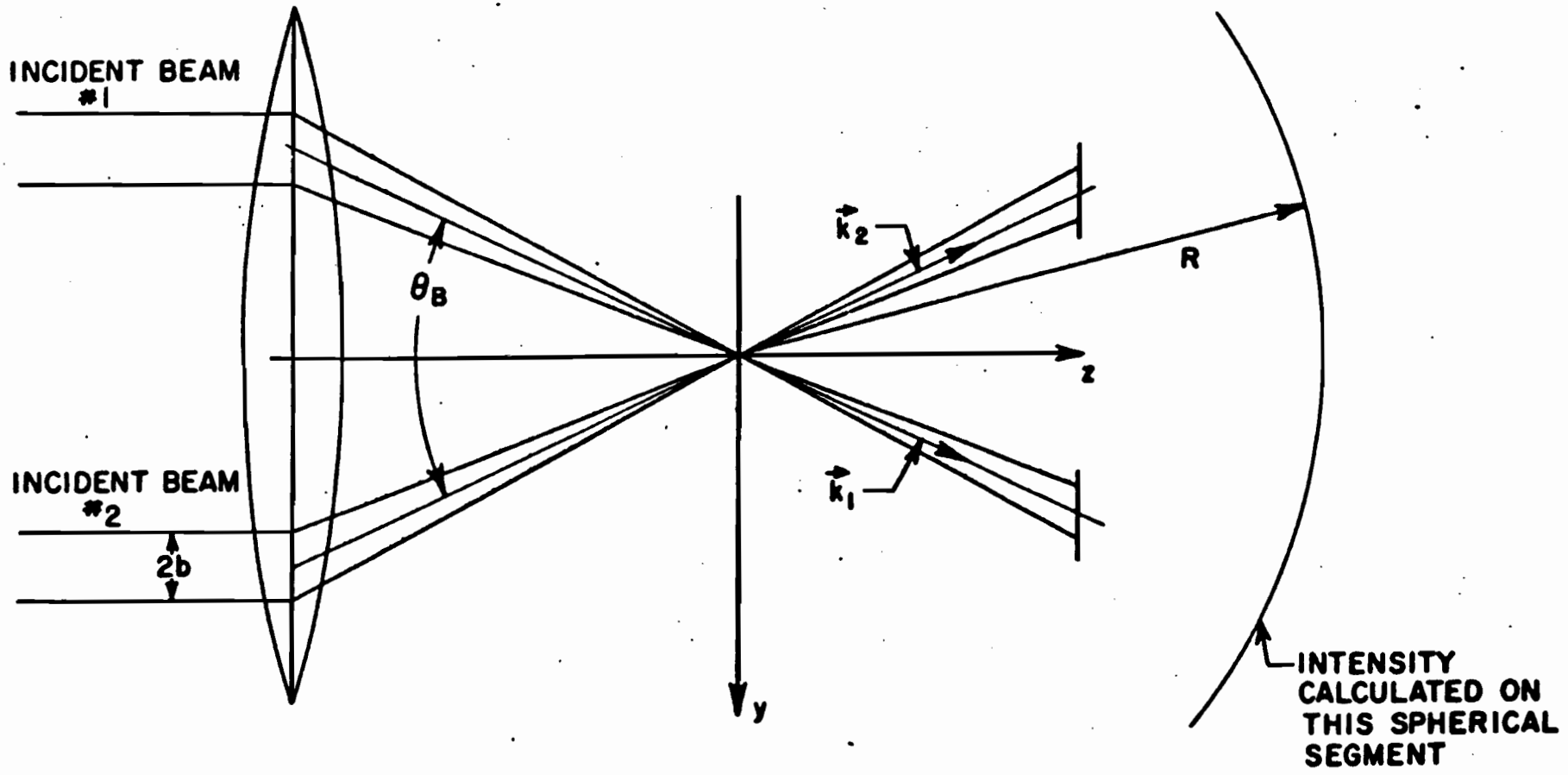

Fig. 10. Dual-Scatter System

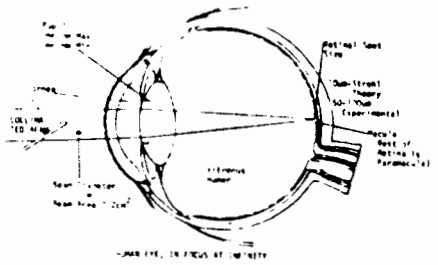

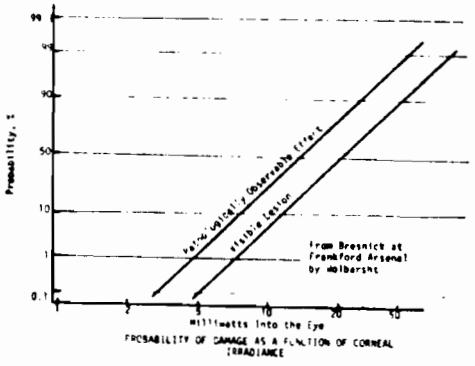

PROBABILITY OF DAMAGE AS A FUNCTION OF CORNEAL IRRADIANCE

LASER SAFETY

1. WEAR LASER SAFETY GLASSES (REMOVE THEM ONLY WHEN THE BEAM POWER IS BELOW 1mw)
2. DO NOT EXPOSE EYES TO DIRECT BEAMS OR SPECULAR REFLECTIONS.

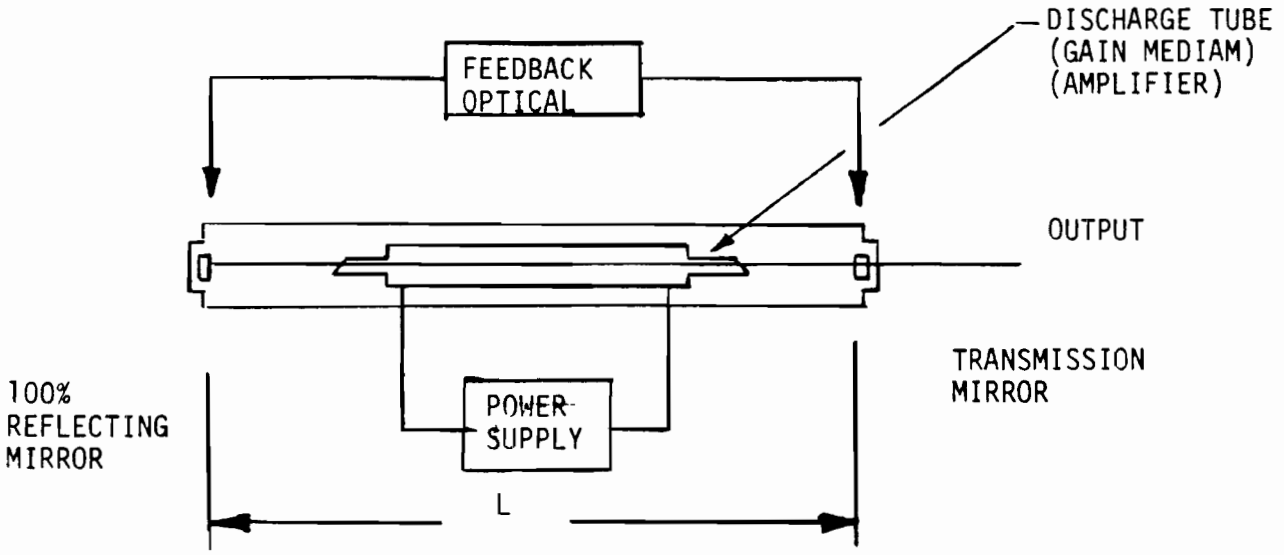

The laser is similar to any oscillator; i.e. R.F. or spring mass. The mirrors form an optical resonator and the discharge tube a means of supplying gain. The amplifier is a glass tube which contains a gaseous mixture which acts as the active lasing material. When the laser's power supply (the "pump") delivers enough energy to cause continous glow discharge in the gas tube (much the same as neon sign is pumped by an electrical discharge), the atoms are elevated to a higher energy state by collisions. When the atoms drop back to their lower energy state, they give up energy at a certain wavelength. The light output will be random and scattered equally in all directions. Some of this light is lost through the side walls of the glass tube, but the portion

that travels down the center of the tube, strikes other excited atoms, creating more light energy of the same wavelength.

The laser tube is placed in an optical cavity formed by two highly reflective mirrors positioned to face each other along a central axis. The mirrors reflect the initial beam which, as it bounces back and forth, eventually builds up enough energy to emerge through whichever mirror has the least reflectivity. This escaping light constitutes the highly directional beam of the laser. Light amplification is only 1.02 on each pass of the beam from one mirror to the other; all losses must be kept below 2%. This so-called transmission mirror is coated to allow less than 1% of the generated light to escape. Thus, the beam emitted is less than 1/100th as intense as the beam between the mirrors.

As the electric energy is applied, the electrons of each atom respond by changing their orbits from the normal ground level configuartion to the larger and more complex orbits associated with higher energy levels. After a short time in the energized state, the electrons spontaneously revert to their original conditions and characteristic spectra these may be observed as each of the atoms radiates its recently acquired energy. When one of the atoms undergoes a particular transition, a photon of light travels down the laser tube and other energized electrons along its path are stimulated to undergo the same transition. This action produces additional radiations of the same frequency. The phenomenon is called stimulated emission or radiation. The stimulated emission

results in a combined wave of increasing amplitude. Upon reaching the end of the laser tube, the wave encounters a mirror which sends it back through the tube to stimulate more energized neon atoms and increase its amplitude by a factor of 1.02 with each pass. With a flar mirror at each end of the laser tube, perfectly aligned waves of high amplitude are generated in a very short time.

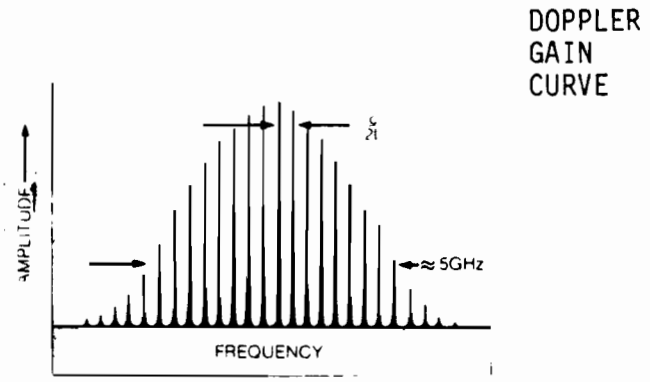

Normal multilongitudinal mode distribution of typical ion laser

Since the laser tube and the mirrors form an optical resonant cavity, the optical path length between successive reflections at a mirror must be of an integral number of wavelengths to produce reinforcement of the wave. Perfect alignment of the mirrors produces a beam which has an irradiance distribution that decreases smoothly from the center to the edge of the beam; the flux density pattern is ideally Gaussian over the beam's crosssection. This pattern, - a single disk area, -produces a single spot of light. This is called the TEM_{oo} mode. (From Tranverse Electric and Magnetic) The cavity has a set of discrete resonant frequencies (longitudinal modes) at

$$f_m = \frac{mC}{2NL}$$

where C is the speed of light, N is the refractive index of the mediam and L is the cavity length.

However the only modes that will be amplified are those within the gain curve of the atomic transition. For a high power laser it is common for numerous modes to be amplified simultaneously.

The difference in frequency between modes is:

$$f_{m+1} - f_m = \frac{C}{2NL} = \frac{3x10^8 m/sec}{2x1.0x2m} = 75 \text{ MHZ}$$

For a laser with L=2.0 meters.

Note: If the LDV siganl is equal to or above 75MHZ, beating between the longitudinal modes- can seriuosly deteriorate the signal to noise ratio.

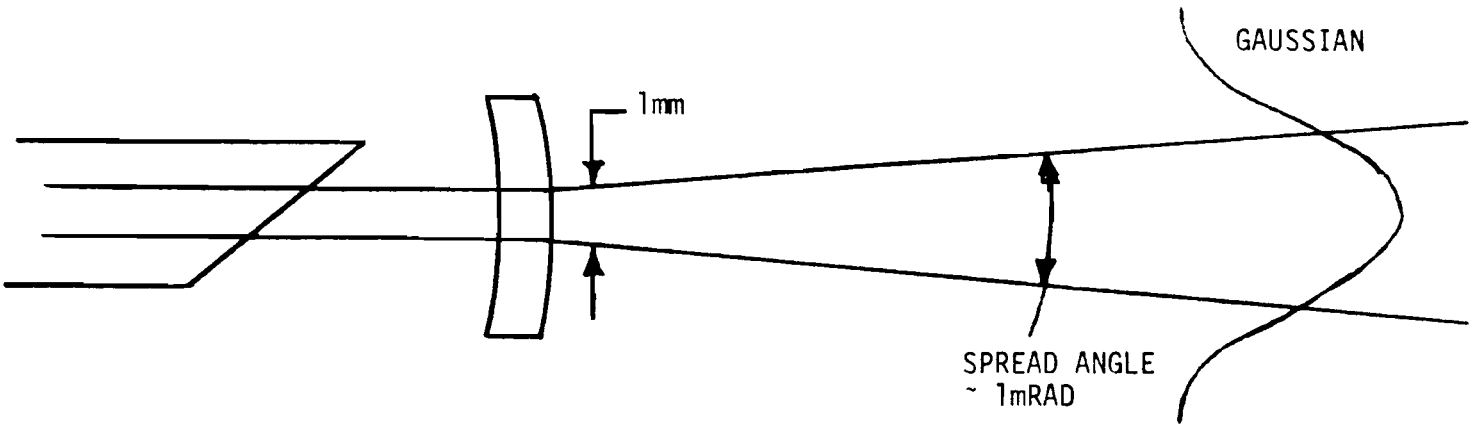

DIA DOUBLES IN
1 METER

Properties of laser light

Laser light is quite different from light normally encountered. It has four unique characteristics that make the device a useful tool: (1) it is highly directional, (2) coherent, (3) very bright, and (4) monochromatic.

1) The directionality of the laser light is because only the light on the axis between the mirrors can escape from the laser. The beam emerges inherently well collimated and highly directional, and thus useful for applications where high concentration of light in a given direction is important.

2) The coherence of laser light in time and space is the one previously unobtainable property that makes it such an important source of light. Only light whose multiples of half a wavelength fit exactly between the mirrors is allowed to escape from the laser. Thus, standing waves are established between the mirrors, and each light particle is in step with the others. Since the light produced by the laser can be thought of as a wave oscillating some 10^{14} times a second, for such a wave to be coherent two conditions must be fulfilled: 1) It must be very nearly a single frequency(the spread in frequency or linewidth must be small). If this condition is fulfilled, the light is said to have temporal coherence, and 2) the wavefront must have a shape which remains constant in time. (A wavefront is defined to be the surface formed by points of equal phase. A point source of light emits a spherical wavefront. A perfectly collimated beam of light has a plane wavefront.) If this second condition holds, the light is said to be spatially coherent.

3) Intensity and monochromaticity go hand in hand. Since the laser builds up energy of only one frequency, all its power per interval of wavelength is much greater than the power available from other sources, this is simply because of its greater monochromaticity.

4) Monochromaticity (single coloredness) is the result of the narrow pass band of the amplifier plus the selectivity of the resonant feedback mirrors. It is possible to limit the

wavelength spread to a small band, say from 1 nm to 10 nm and produce light of high chromatic putiry. Such light is called roughly "monochromatic" light, meaning light of a single color.

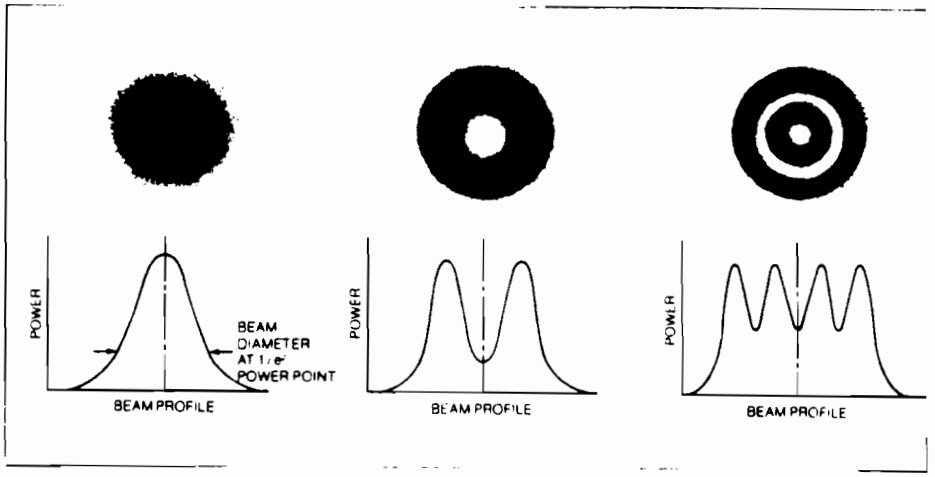

TEM_{oo} fundamental or Gaussian mode

TEM_{oo} first order or donut mode

Typical higher order multitransverse mode

The TEM_{oo} mode has a number of properties which make it the most desirable mode in which to operate. The TEM_{oo} beam's angular divergence is smallest and can be focused down to the smallest sized spot. Futhermore, the TEM_{oo} (uniphase!) mode does not suffer any phase shifts or reversals across the beam as do higher order modes. It is completely spatially coherent. This is an important consideration in interferometric applications and holigraphy.

However, other modes such as those shown above can occur, usually due to laser misalignment or dirt on the mirrors. A particular troublesome mode is the "doughnut mode" that occurs in the 4880$\AA$ line of the Argon Ion Laser.

ARGON ION LASER PROPERTIES

Spectra-Physics Model 171-09
Beam Diameter = 1.6mm
Beam Divergence = .6mrad
(Full Angle)
Polarization = Linear-Vertical
Mode Spacing ~ 87 MHZ

ARGON ION LASER POWER, TEM_{oo}

Wavelength (nm) Multi-Line	Model 171 -09
457.9-514.5	18 watts
Single-Line	
514.5	7.5
501.7	1.5
496.5	2.5
488.0	6.5
476.5	2.7
472.7	1.2
465.8	.75
457.9	1.35

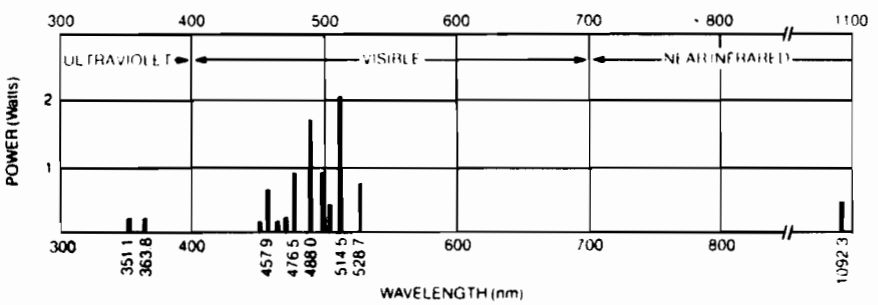

Typical lasing wavelengths and relative power levels from a 4 Watt size Argon laser*

ETALON

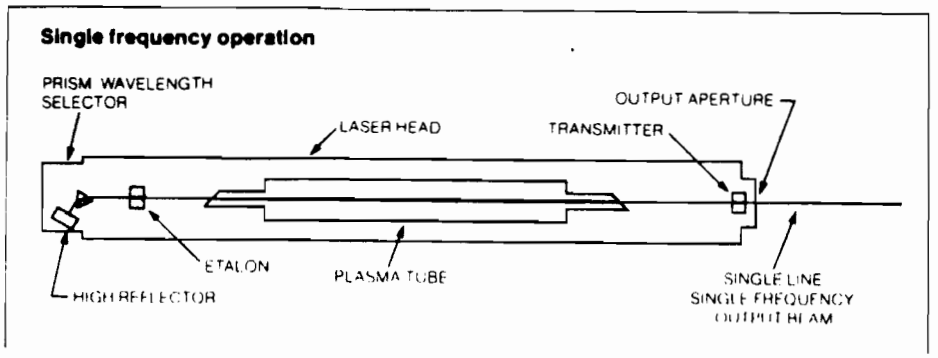

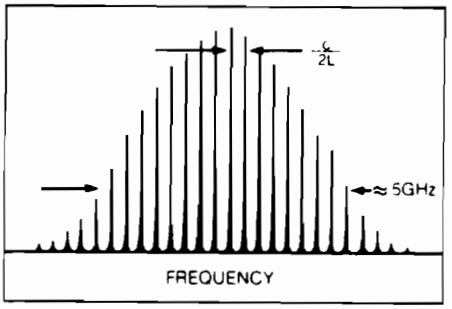

Normal multilongitudinal mode distribution of typical ion laser

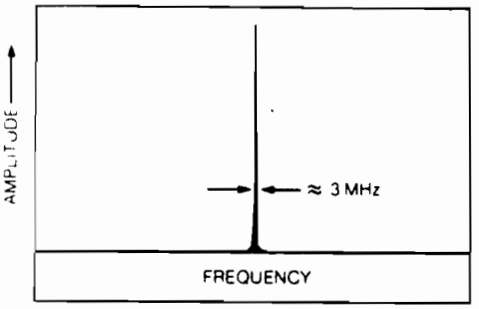

Single longitudinal mode (or single frequency) output of ion laser using an etalon

COHERENCE LENGTH

$$= \frac{3\times10^{8}\text{m/sec}}{5\times10^{9}/\text{sec}}$$

$= 6\text{cm}$

COHERENCE LENGTH

$$= \frac{3\times10^{8}\text{m/sec}}{3\times10^{6}}$$

$= 100\text{m}$

The intercavity etalon provides a means of reducing the number of longitudinal modes to one, thus increasing the coherence length of the emitted light. This also eliminates beating of the longitudinal modes which can be a source of noise at higher frequencies in LDV systems.

The Fabry-Perot consists of two optically flat partially reflecting plates of glass or quartz (with their reflecting surfaces held accurately parallel.) Multiple beam interference increase the laser loss for all frequencies under the gain curve except one.

POLARIZATION - BREWSTER'S ANGLE

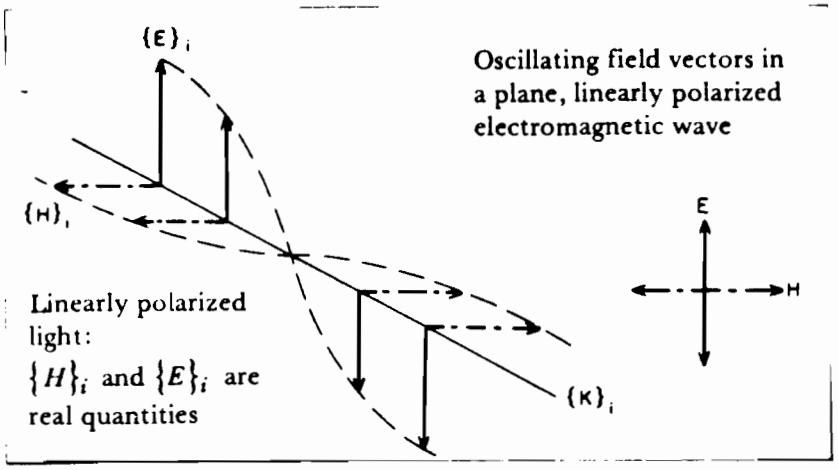

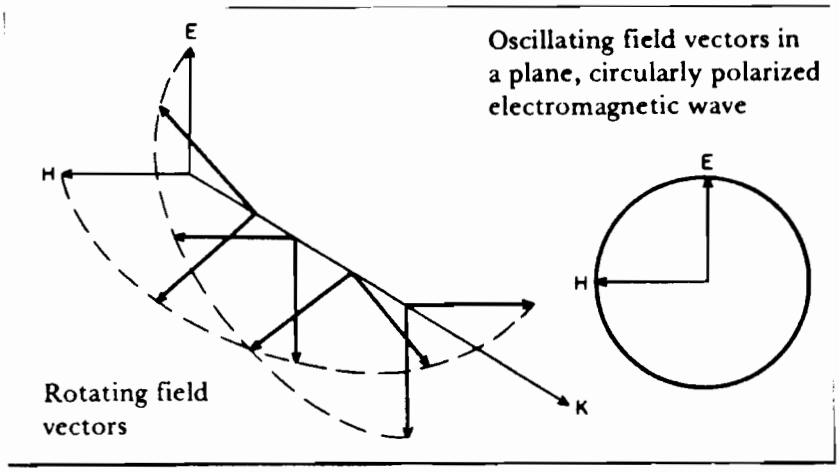

REFLECTED POWER = 0
FOR LIGHT THAT IS LINEARLY
POLARIZED IN THE PLANE
OF THE PAPER

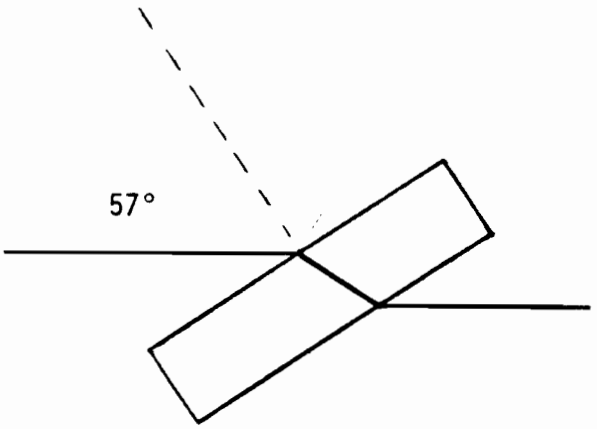

All laser light is polarized. The total output power of a "linearly polarized laser" lies in a single defined plane of polarization. This state of polarization is caused by the "Brewster" windows at the end of the laser tube. At Brewster's Angle with incident radiation polarized parallel to the incendent plane there is no reflected light. The incident field gives rise to vibrations of electrons in the atoms of the second medium. These vibrations are in the direction of the electric vector of the transmitted wave. The vibrating electrons give rise to another wave, the reflected wave which will be propagated back into the first medium. A linear vibrating electron (dipole radiator) radiates trans-

versally so there is no flux of radient energy in the direction of vibrations. So when the reflected wave and transmitted wave are perpendicular the reflected wave recieves no energy. Circularly polarized light occurs when two light waves of the same amplitude, linearized polarized at right angles to each other and having a 90° phase shift between them are combined. Combining waves with a different amplitude or phases results in elliptic polarization.

In the case of natural light, random fluctuations in the direction of oscillation of the electric field are observed and the light wave is said to be unpolarized. The randomness of the charge in the direction of oscillators is characteristic of natural light emitted by thermal light sources.

MIRRORS -PRISM- BEAMSPLITTERS

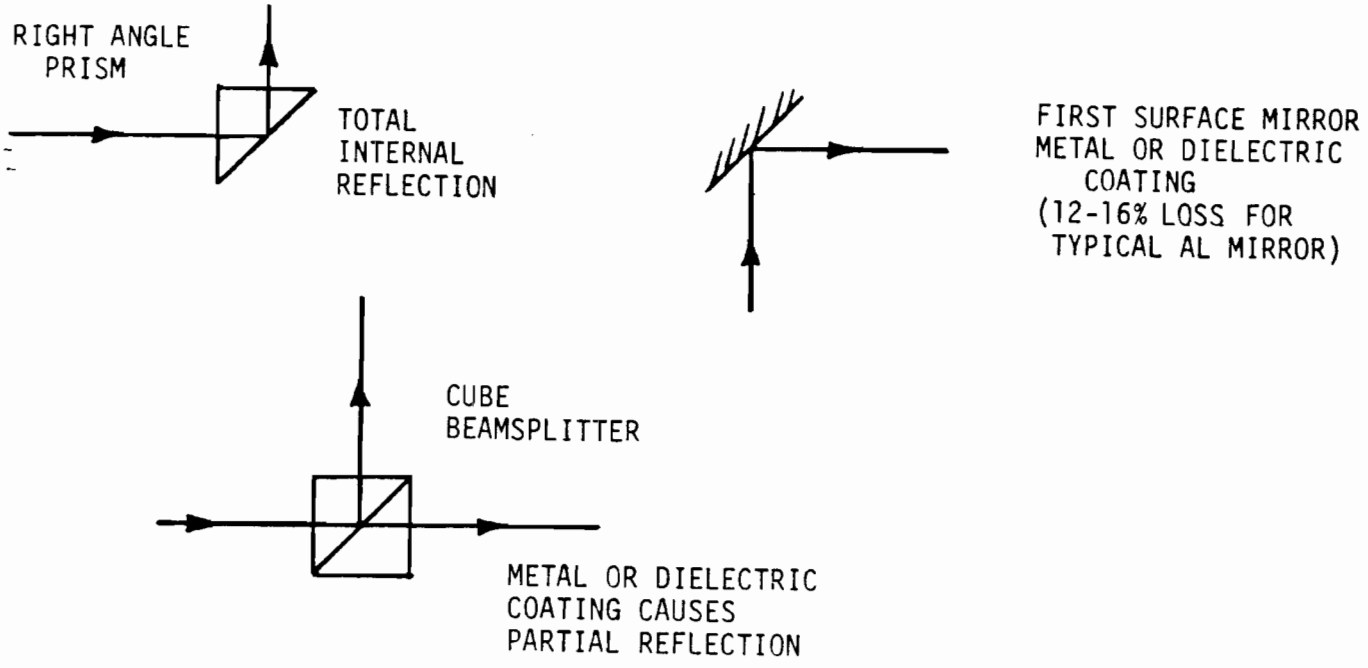

Mirrors and beamsplitters are usually polarization sensitive. That is their reflectence depends on the state of polarization of the incident wave. This is of particular importance in LDV, since an improper polarization state can lead to unequal beam intensities after the beamsplitter. As shown later this causes poor fringe visibilty.

THIN LENSES

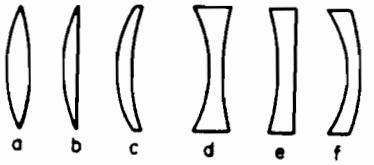

a bi-convex lens
b plano-convex lens
c convex-concave lens
d bi-concave lens
e plano-concave lens
f concave-convex lens

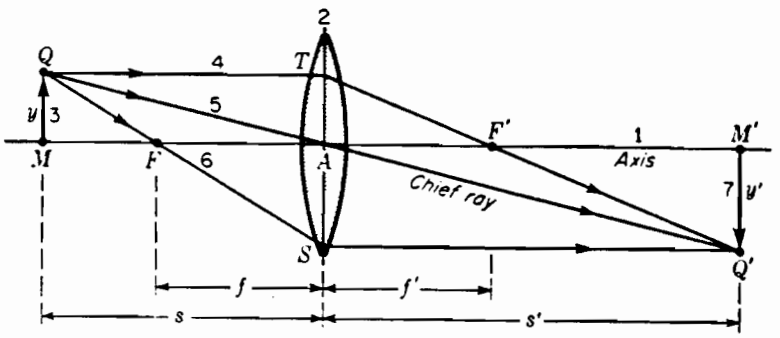

$$\frac{1}{S} + \frac{1}{S'} = \frac{1}{f}$$

$$M = \frac{y'}{y} = -\frac{S'}{S}$$

Use in LDV for determining the proper size of pinhole in the recieving optics.

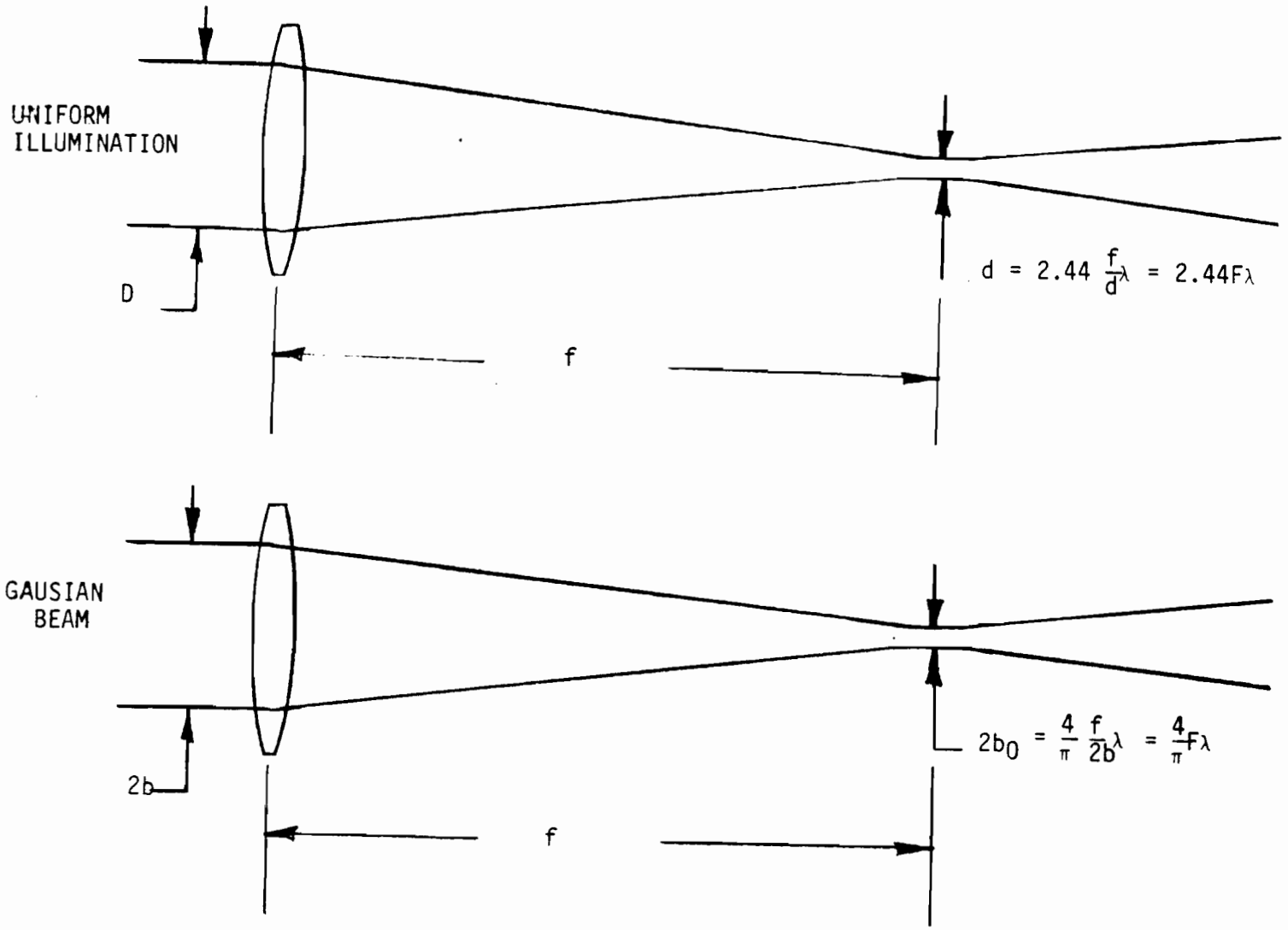

When a beam of light passes through an aperature, i.e. circular, rectangular, slit etc., it spreads out to a certain extent into the region of the geometrical shadow. This effect is one of the simplest examples of diffraction, i.e., of the failure of light to travel in straight lines. It can be satisfactorily explained only by assuming a wave character for light.

OPTICAL FILTERS - AR COATINGS

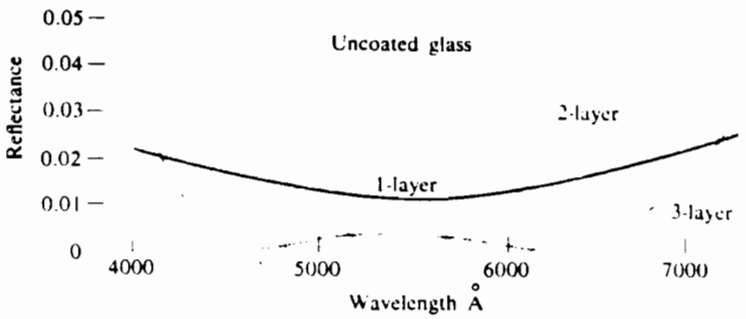

Curves of reflectance versus wavelength of antireflecting films.

Multilayer Fabry-Perot interference filter.

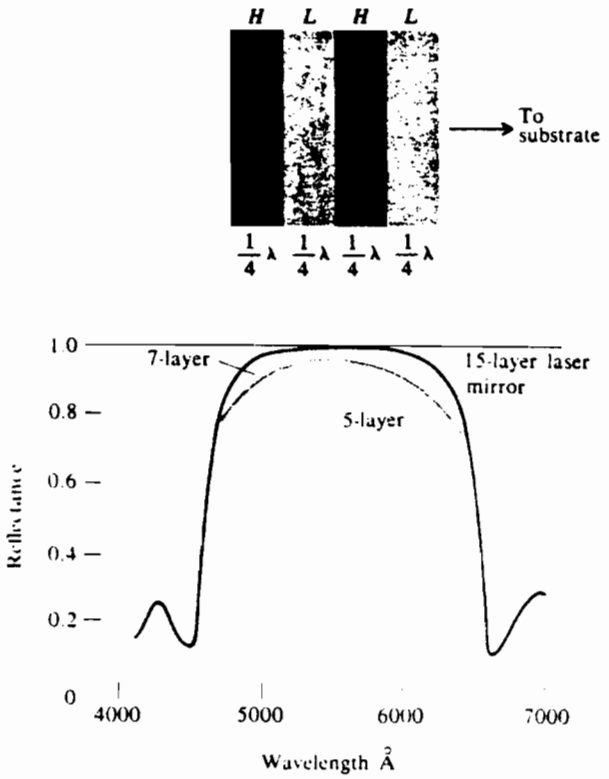

Reflectance curves for some multilayer high reflectance films.

Multi-layer dielectric films that are vacuum deposited on glass are used as optical filters, anti-reflection coatings and laser mirrors. Alternate layers of high and low index of refraction material allow the optical designer to use multibeam interference to produce the desired properties. In effect, this is a Fabry-Perot etalon with a very small spacing. The result is a filter that has a transmission curve given by the Airy function.

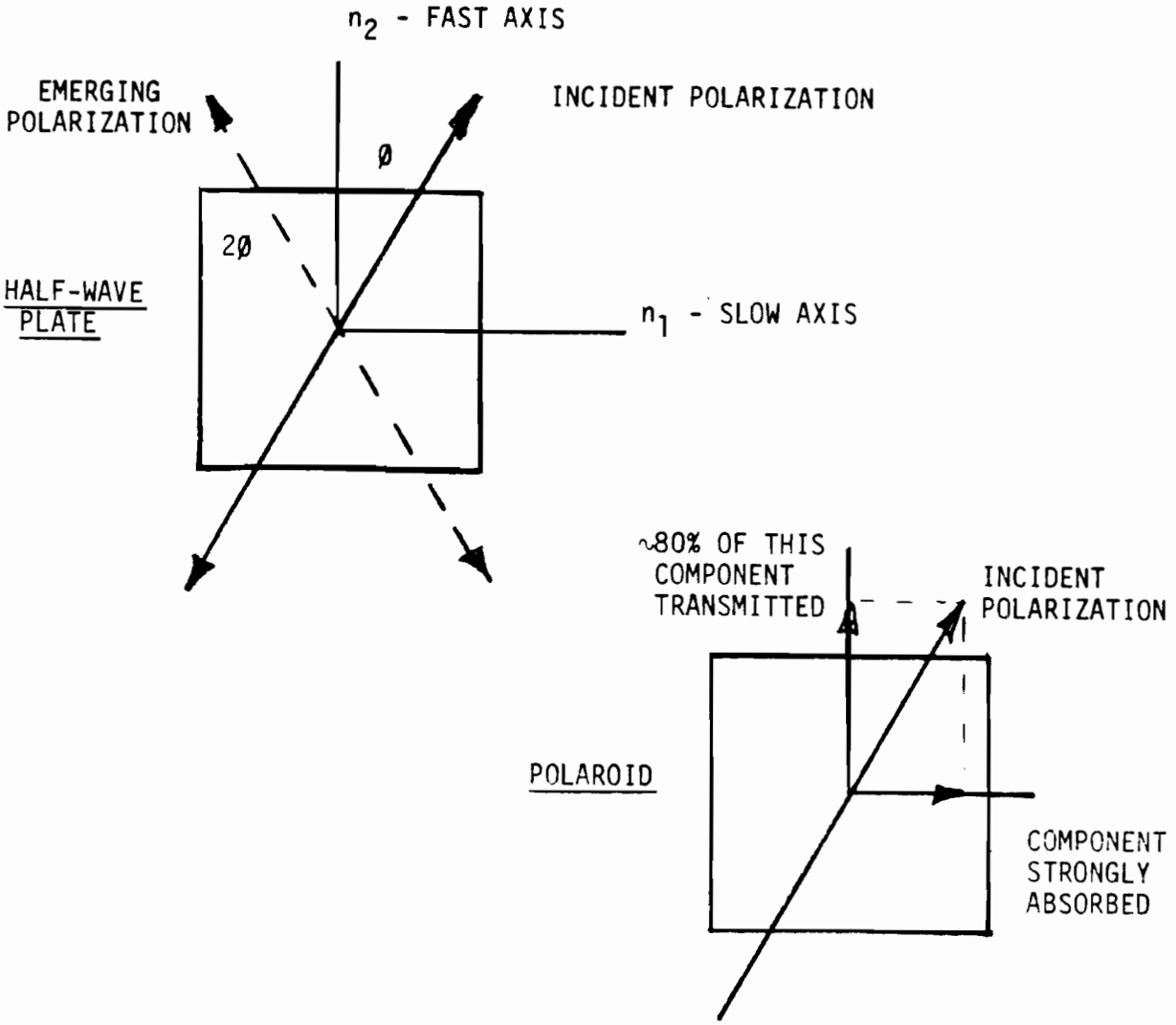

Wave plates and polaroids are device used for changing or analyzing the polarization of an incident light beam.

Wave plates are made of doubly refracting (or birefringent) transparent crystals such as mica or quartz. The polarization produced in the crystal depends on the direction of the applied field in relation to the crystal lattice. One of the consequences is that the speed of propagation of a light wave in a crystal is a function of the direction of propagation and polarization of the light.

A half wave plate is used to rotate the plane of vibration of linearly polarized light. A crystal (mica or quartz) is cut

in such a way that an axis of maximum index n_1, (the slow axis) and an axis of minimum index n_2 (the fast axis) both lie at right angles to one another in the plane of the slab. The thickness of the half wave plate is chosen so that there is 180° phase shift the fast and slow components of the incident light. Therefore

$$d = \frac{\lambda}{2(n_1 - n_2)}$$

The results as shown in the diagram is that the output polarization is still linear but the plane of polarization is rotated by an angle 2 Ø with respect to the crystal axis.

A quarter wave plate is piece of the same type of material but only half as thick

$$d = \frac{\lambda}{4(n_1 - n_2)}$$

When linearly polarized light is incident at 45° to the crystal axis, a 90° phase shift between the fast and slow components occurs. This results in circularly polarized light.

"Polaroid" material is composed of aligned long chain molecules (iodine or polarized alcohol) resulting in an absorbtion coefficient that is dependent on the incident polarization. The ratio of absorbtion coefficients may be as high as 100:1.

Photomultiplier Tube

Tube: RCA 4526

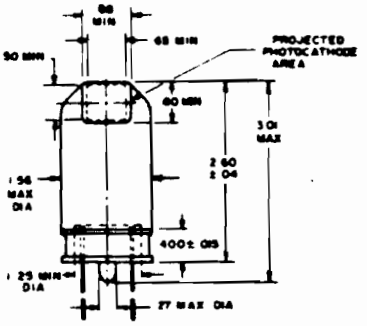

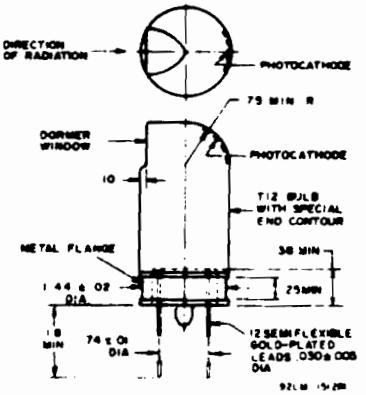

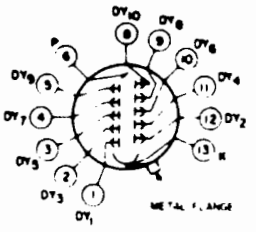

Maximum Ratings	Typical Characteristics at the Supply Voltage and Distribution Specified and at 22°C					
			Sensitivity			
Supply Voltage V	Average Anode Current mA	Supply Voltage V	Radiant Cathode mA/W	Radiant Anode A/W	Luminous Cathode uA/lm	Luminous Anode A/lm
2000	0.10	1250	89	4,400	300	15

Anode Pulse Rise Time ns	Anode Dark Current nA @ Anode Luminous Sensitivity	Remarks	Dynode Secondary Emitting Surface Material
1.7	2@20	Multialkali photocathode	Be-O-Cs

LASER SPECKLE

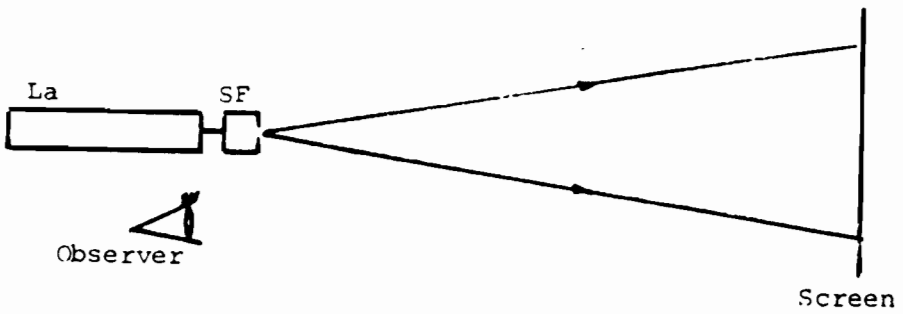

Although not used in LDV, laser speckle is always observed during alignment. Laser light is diffusely reflected as a set of spherical waves from points of the surface. These spherical waves interfere with each other to produce the dot pattern called speckle. When the observer's head is moved extremely slowly from side-to-side while looking at the illuminated area on the screen, the speckle pattern appears to move.

If the movement of the speckle pattern is in the same direction as the relative movement between the observer and the screen (that is, if the observer's head moves to the right and the speckle pattern also appears to move to the right), the eye is hyperoptic (farsighted).

If the movement of the speckle pattern appears to be in the opposite sense, the eye is myopic (nearsighted).

If there is no speckle movement observed the eye is emmetropic (normal). A person who normally wears eyeglasses should take this test with and without the glasses. In case of astigmatism the apparent movement of the speckle pattern will depend on the refractive condition of the eye in the plane of the movement. For example, at some diagonal movement of the head the speckles will remain stationary, up and down tilt of the head will produce speckle movement in the opposite sense, and sideways motion will result in speckle movement in the same sense. This example indicates mixed astigmatism, that is, the eye is myopic in the vertical meridian, hyperopic in the horizontal meridian and emmetropic at some diagonal direction.

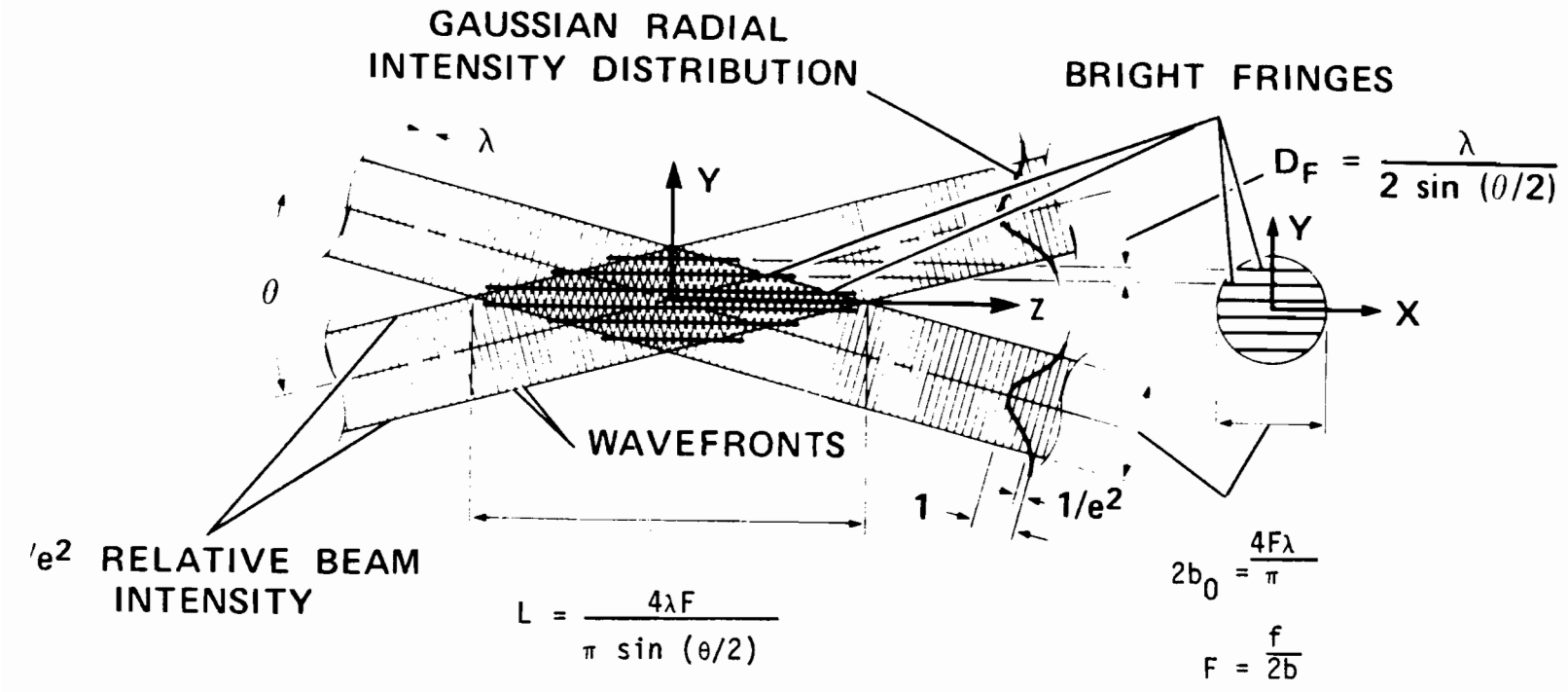

When two coherent beams of light of the same frequency intersect they will form a set of real interference fringes. The intersection of the two plane waves of the same intensity and polarization shown above, produce a set of straight highly visible interference fringes.

The dual beam LDV system measures the component of the velocity vector lying in the plane of the beams and perpendicular to the bisector of the beams.

$$\text{frequency} = f = \frac{U}{D_f} = \frac{2U \sin \Theta/2}{2}$$

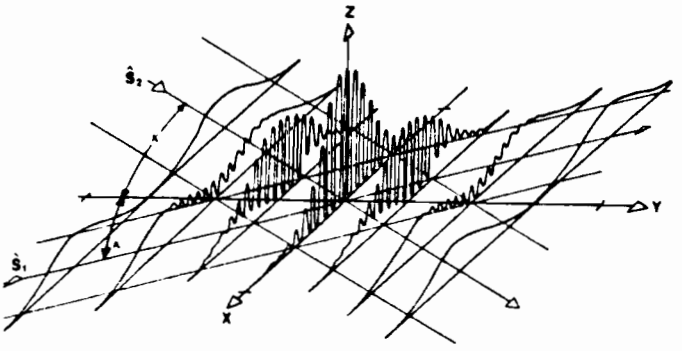

THE RELATIVE INTENSITY DISTRIBUTION NEAR THE CROSSOVER OF TWO EQUAL POWER, SIMILARLY POLARIZED, GAUSSIAN LASER BEAMS.

The intensity distribution of two intersecting waves is given by:

$$\vec{E}_1 = \vec{E}_{0_1}(\vec{r})\ e^{i(\omega t - \vec{k}_1 . r)}$$

$$\vec{E}_2 = \vec{E}_{0_2}(\vec{r})\ e^{i(\omega t - \vec{k}_2 . \vec{r})}$$

$$I = (\vec{E}_1 + \vec{E}_2)\ .\ (\vec{E}_1 + \vec{E}_2)^*$$

$$I = \left|\vec{E}_{0_1}\right|^2 + \left|\vec{E}_{0_2}\right|^2 + 2\vec{E}_{0_1} \cdot \vec{E}_{0_2}\ \cos\ 2\pi\left(\frac{2\sin\Theta/2 y}{\lambda}\right)$$

The optimum case occurs when the magnitude of the two waves is equal ($\left|\vec{E}_{0_1}\right| = \left|\vec{E}_{0_2}\right|$) and the two waves the same polarization state ($\vec{E}_{0_1} = \vec{E}_{0_2}$) then

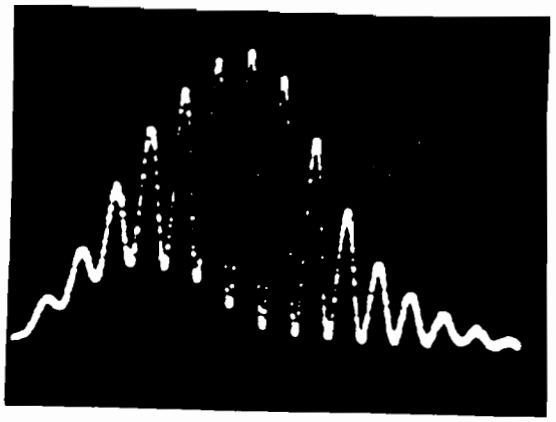

EQUAL INTENSITY BEAMS

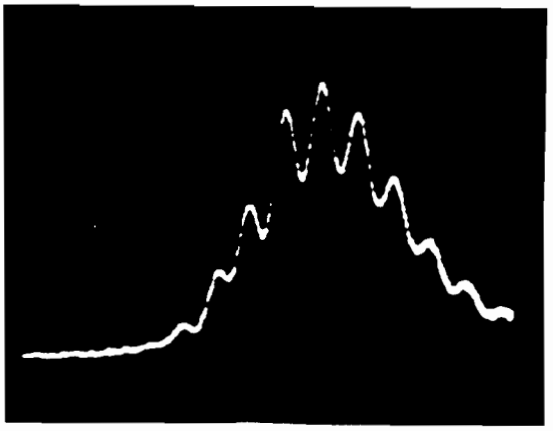

A.C. COMPONENT

PEDASTAL

UNEQUAL INTENSITY BEAMS

$$I = 2\left|\vec{E}_{0_1}\right|^2\left(1 + \cos 2\pi\left(\frac{2\sin\theta/2y}{\lambda}\right)\right)$$

The intensity distribution oscillates from $4\left|\vec{E}_{0_1}\right|^2$ to 0 thus giving rise to a set of interference fringes. Note that if either the magnitude or polarization of the two wave is different then the excursions of the intensity will not be as great. (i.e. the fringes will not be as distinct) For instance if

$\vec{E}_{0_2} = 1/2\ \vec{E}_{0_1}$

$$I_0 = \left|E_{0_1}\right|^2\left(5/4 + \cos 2\pi\left(\frac{2\sin\theta/2y}{\lambda}\right)\right)$$

The intensity oscillates from 2.25 to .25

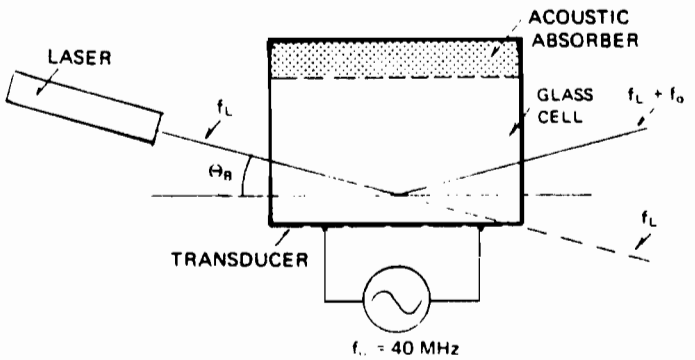

Upshifting or downshifting of the frequency of light waves is possible by means of an accousto-optical device known as a Bragg cell, based on the fact that ultrasonic energy propagating through a liquid medium forms variations in the liquid's index of refraction.

The conventional dual-scatter LDV system yeilds the same siganl for particle velocities that are equal in magnitude but opposite in direction. This 180° direction ambiguity can be resolved by frequency shifting one of the beams using a Bragg cell. This causes the fringes to have a velocity porportional to the frequency shift. Thus a stationary particle will leave a frequency equal to the shift frequency while a particle mov-

ing opposite to the fringes will have a frequency equal to the shift frequency plus the doppler frequency. A particle moving in the same direction as the fringes will have a frequency equal to the shift frequency minus the doppler frequency.

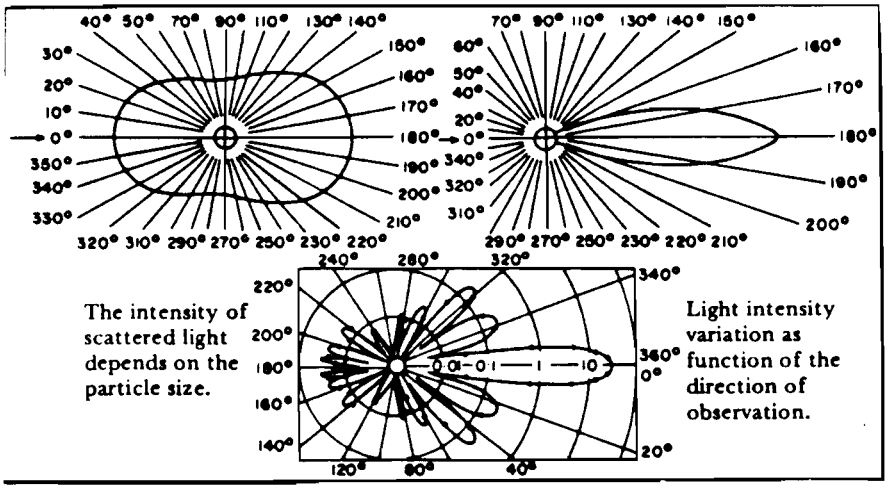

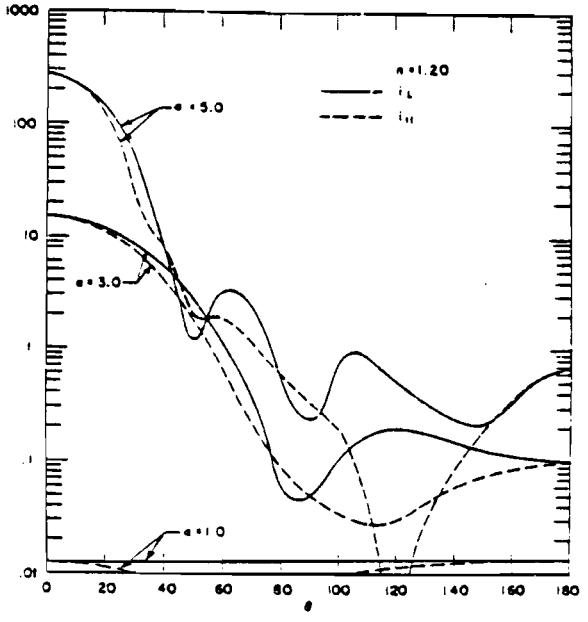

The scattering of light by spherical particles is governed by Mie theory. Some examples shown above indicate the complexity of distribution of scattered light. For normal LDV applications, $\alpha = \frac{\pi d}{\lambda} \simeq 5$, the light scattered in the forward direction is two orders of magnitude higher than that scattered in the backwards direction. This is easily observed when a laser beam passes through a smoke cloud. The beam appears more intense when viewed in the forward scattering direction than when viewed in the backscatter direction.

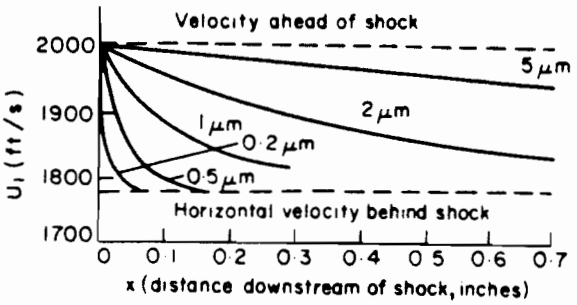

Recovery distance for particles across oblique shock.

PARTICLE DIAMETER (μm)	RELAXATION TIME (sec)
0.5	7.7×10^{-7}
0.6	1.1×10^{-6}
0.7	1.5×10^{-6}
0.8	2.0×10^{-6}
0.9	2.5×10^{-6}
1.0	3.1×10^{-6}
2.0	1.2×10^{-5}
3.0	2.8×10^{-5}
4.0	4.9×10^{-5}
5.0	7.7×10^{-5}

The presence of the right type of particles in the flow is vital for successful LDV measurements. The requirements are:

1. They should follow the flow adequately
2. They must scatter sufficient light to produce measurable signals
3. They should be present in desirable numbers

The relaxation time $\tau = \frac{\rho_p}{\rho_f} \frac{d_p^2}{18 \nu_f}$ is a measure of the time it will take for a particle to respond to a step change in velocity.

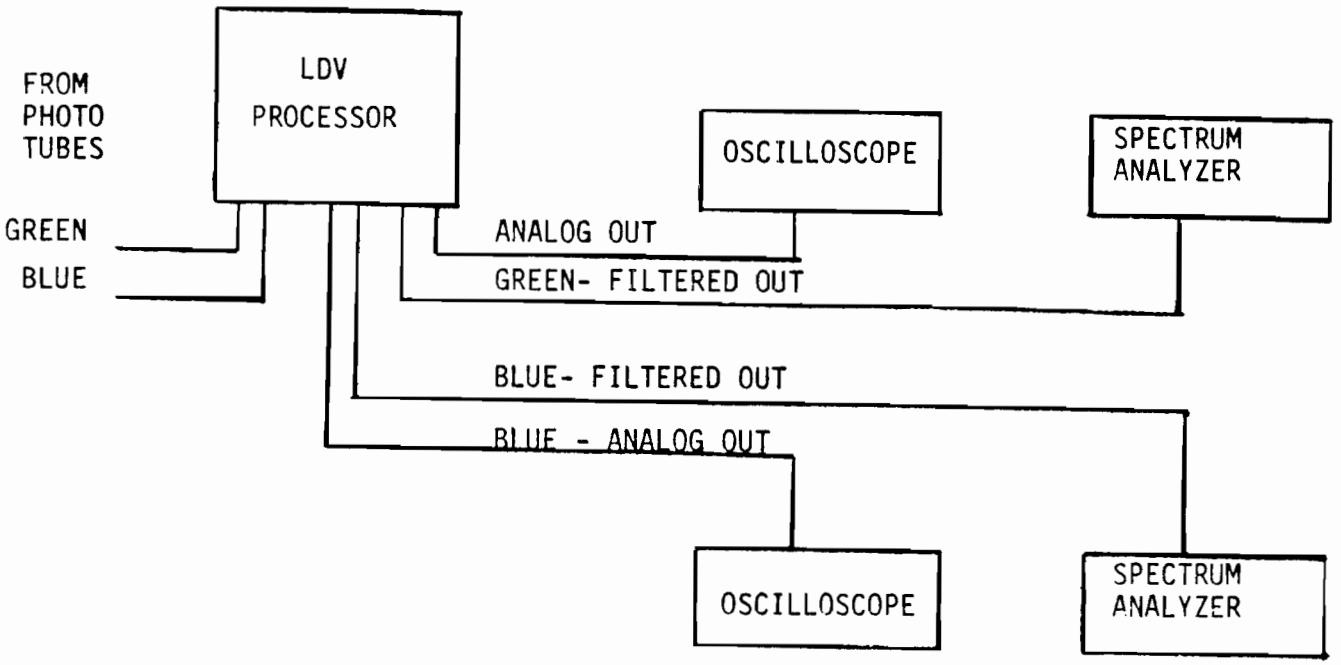

The signal from the two photomultiplier tubes is connected to the LDV Counter Processors. The processors filter and amplify the LDV burst and then count the time for a fixed number of cycles of the doppler frequency. A digital signal proportional to one over frequency is sent to the computer and an analog signal also inversely proportional to the frequency is displayed on an oscilloscope.

Monitoring the analog output of the processor and the filtered LDV signal (using the spectrum analyzers) is crucial for assessing system performance during any test.

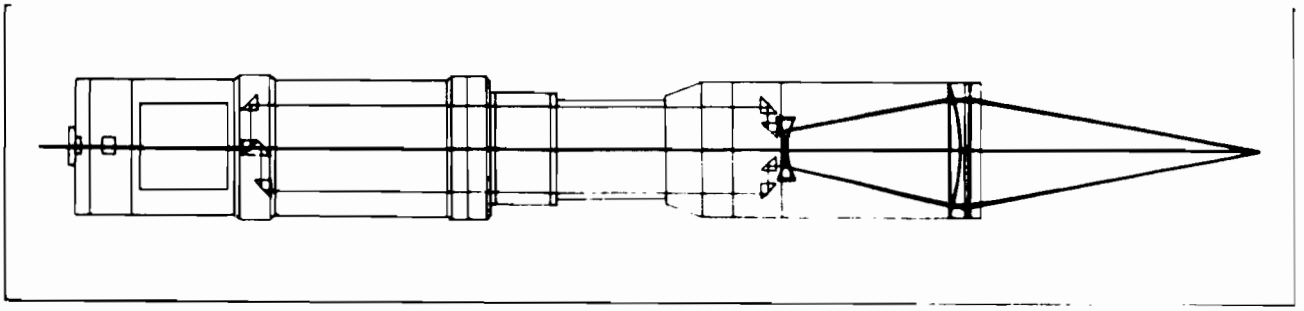

Fig. 13. Transmitter Beam Path.

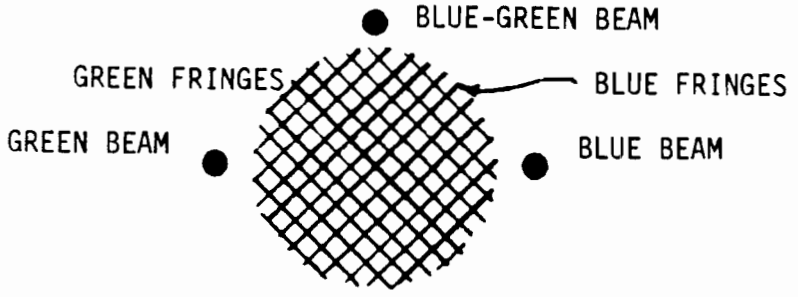

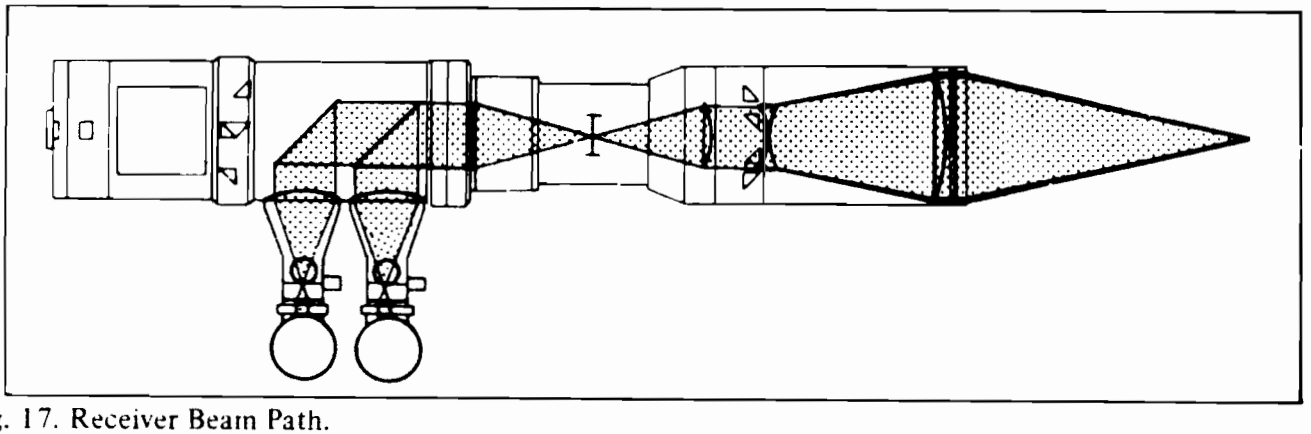

Fig. 17. Receiver Beam Path.

TWO TWO-COLOR SYSTEM

The two-color LDV utilizes the two strong laser lines of an Ar-ion laser at 488 nm (blue) and 514 nm (green) to form a two-channel fringe system. These two colors, which are of about the same power, are separated in the optical system and emitted from the optical system in such a way that two orthogonal fringe systems, one formed by the blue beams and the other by the green beams, are formed in one common focal volume.

LDV FORMULAE

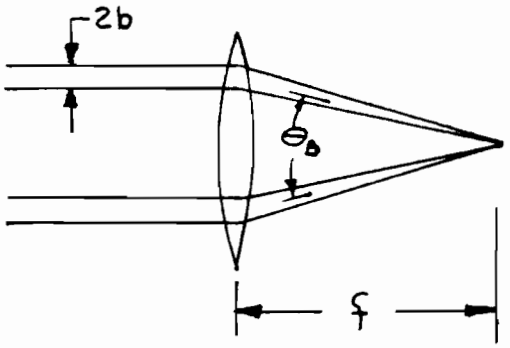

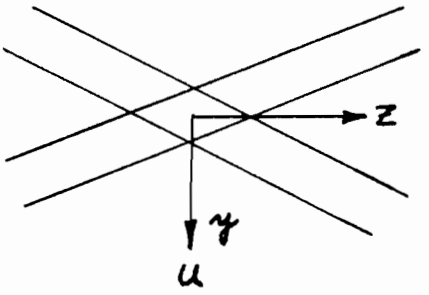

b = radius of input beam ($1/e^2$ Intensity)

f = focal length of lens

θ_B = angle between beams

$$f_D = \frac{2U \sin \theta_B/2}{\lambda} = \text{frequency}$$

$$N = \frac{2F \tan \theta_B/2}{\pi} = \text{number of fringes}$$

$$F = \frac{f}{2b}$$

$$b_o = \frac{2F\lambda}{\pi} = \text{radius of focused beam to } 1/e^2 \text{ intensity points}$$

$$\ell = \frac{2b_o}{\sin \theta_B/2} = \frac{4\lambda F}{\pi \sin \theta_B/2} = \text{length of probe volume}$$

$$\text{Fringe Spacing} = \frac{\lambda}{2 \sin \theta_B/2}$$

$$\left(\frac{x}{b_o}\right)^2 + \left(\frac{y}{b_o/\cos \theta_B/2}\right)^2 + \left(\frac{Z}{b_o/\sin \theta_B/2}\right)^2 = 1$$

Equation for Probe Volume ($1/e^2$ Intensity)

Worksheet for Preliminary Design of an LDV System

1. From system constraints choose

$$\lambda =$$

Maximum Working distance = f =

Maximum velocity = U =

Maximum frequency of electronics = f_D =

2. Determine θ_B from graph of f_D vs. U

$$\theta_B =$$

3. From laser manufacturer data determine input beam diameter

$$2b =$$

Calculate $F = \frac{f}{2b}$ =

Determine the number of fringes from graph of N vs. F

$$N =$$

Note - If N is too large (determined by electronics), b can be increased using a colimator which reduces the probe volume and increases the intensity.

If N is too small, θ_B must be increased implying the maximum velocity must be lowered.

4. Determine the length of probe volume from graph of ℓ vs. F.

$$\ell =$$

The diameter of the probe is determined from the same graph with $\theta_B = 180$ (since $\ell = 2b_o$ for $\theta_B = 180°$).

Diameter = $2b_o$ =

If the probe volume is too large it may be reduced by increasing b, which reduces the number of fringes.

The length can be reduced by increasing θ_B, reducing the maximum velocity and increasing the number of fringes.

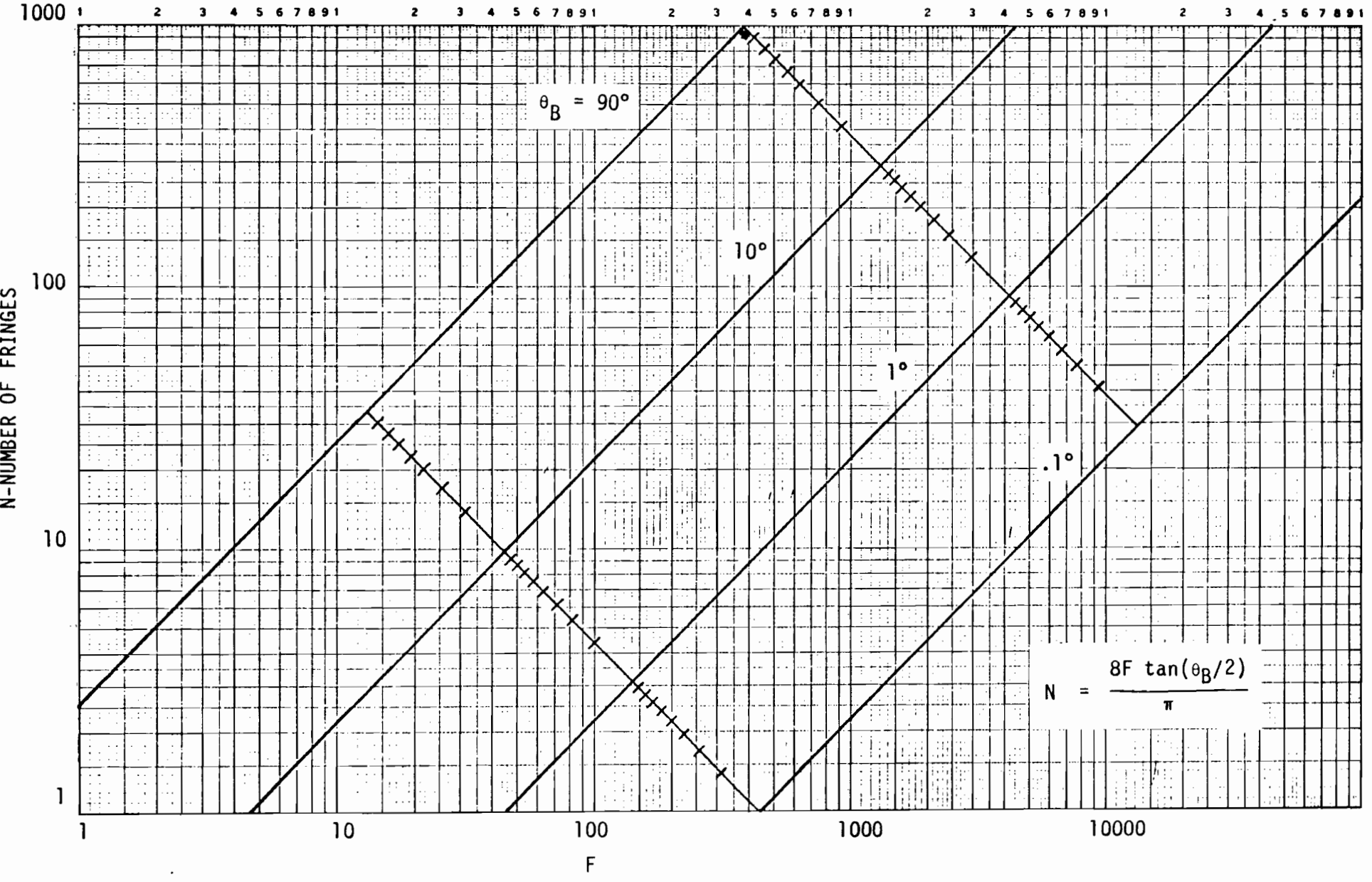

NUMBER OF FRINGES vs F NUMBER.

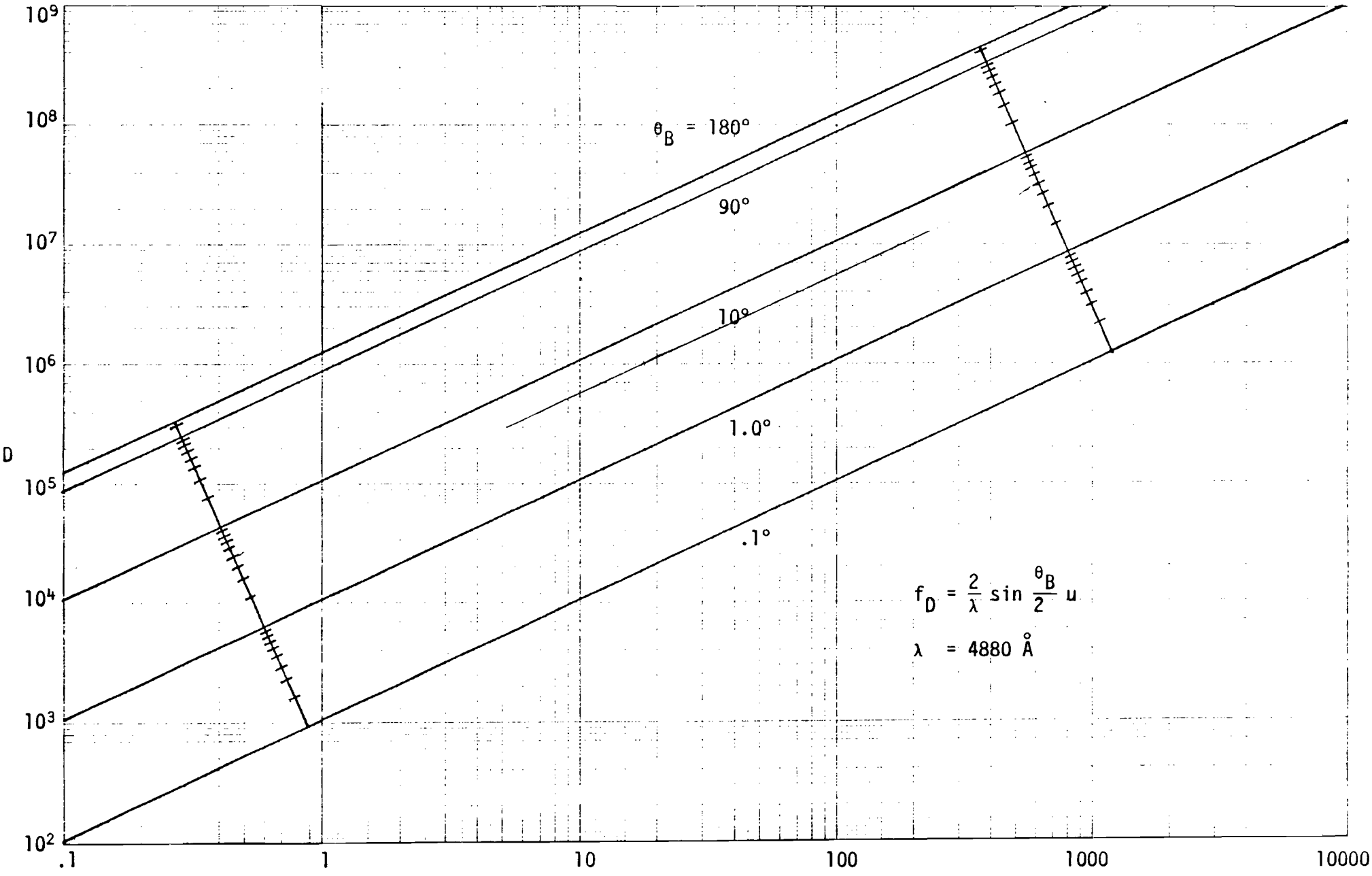

FREQUENCY vs. VELOCITY

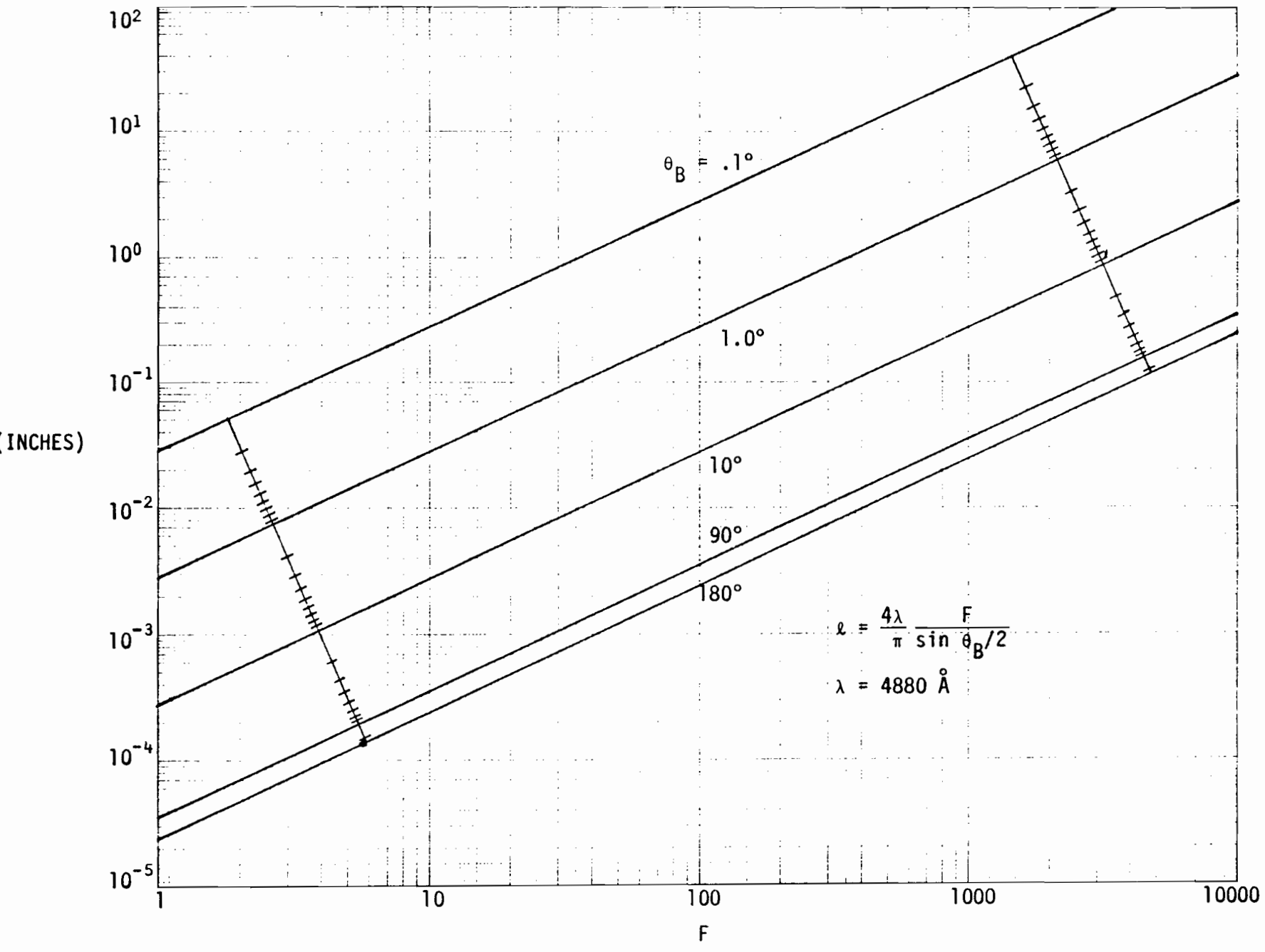

PROBE VOLUME SIZE vs F NUMBER

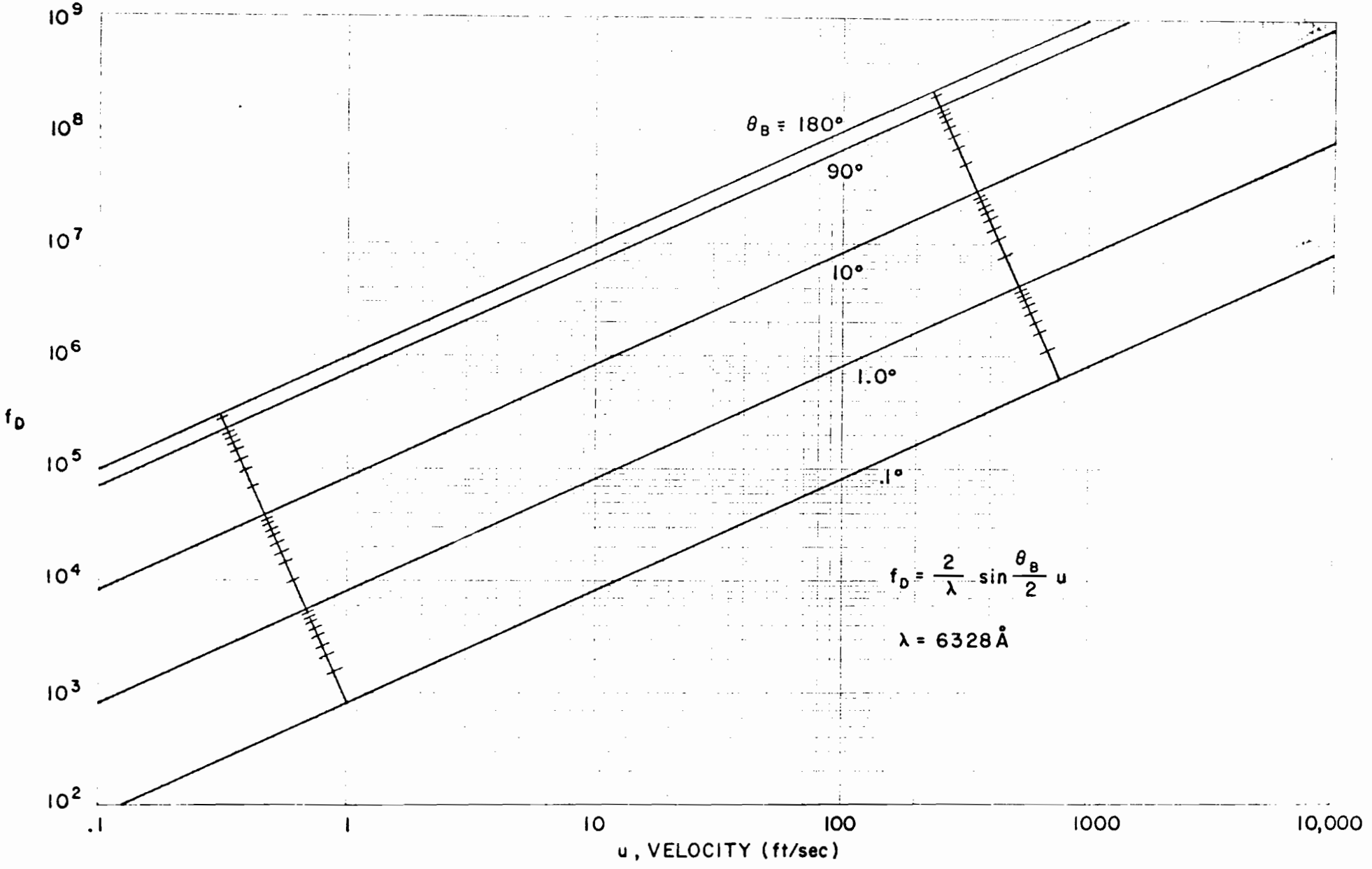
10^9
10^8
10^7
10^6
10^5
10^4
10^3
10^2
f_D
θ_B = 180°
90°
10°
1.0°
.1°
$f_D = \frac{2}{\lambda} \sin\frac{\theta_B}{2} u$
λ = 6328 Å
.1
1
10
100
1000
10,000
u , VELOCITY (ft/sec)

LIST OF REFERENCES

1. Born, M. and Wolf, E. (1964) Principles of Optics, Oxford: Permagon.

2. Durrani, T.S. and Greated, C.A. (1977) Laser Systems In Flow Measurement, Plenum Press.

3. Durst, F., Melling, A. and Whitelaw, J.H. (1976) Principles and Practices of Laser-Doppler Anemometry, Academic Press.

4. Fowles, G.R. (1968) Introduction To Modern Optics (New York: Holt, Rheinhart and Winston).

5. Jenkins, F.A. and White, H.E. (1957) Fundamentals Of Optics, New York: McGraw-Hill.

6. Stevenson, W.H. and Thompson, H.D. (Editors)(1979) "Laser Velocimetry and Particle Sizing", Proceedings of the Third International Workshop on LaserVelocimetry, Purdue University, July. Published by Hemisphere Publishing Corp., Global Bldg., 1025 Vermont Ave. N.W., Suite 1000, Washington, DC 20005.

7. Van deHulst (1957) Light Scattering Small Particles (New York: Wigley).

OPTICAL ALIGNMENT

The optical alignment of an LDV system requires the following:

1. Alignment of the transmitted beams so there is no vignetting. (i.e. the beams do not cut the edges of the prisms or optical package)
2. Overlap the beams at the focal point of the zoom lens to obtain high contrast fringes.
3. Center the image of the probe volume in the pinhole.

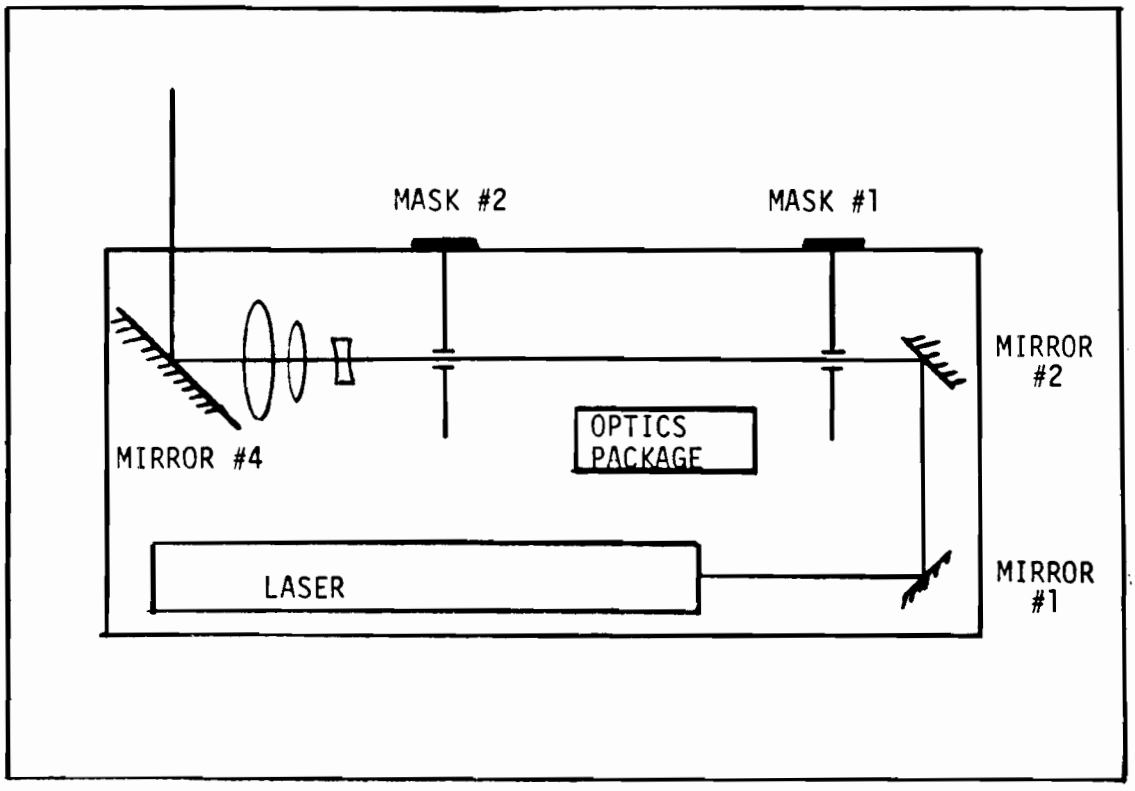

1. Turn on laser as per standard procedure (safety glasses on). Let laser stabilize (approx. 5 min.). Make sure photo-tubes are turned off.
2. Change laser to light mode and set power to 1 watt. Adjust attenuators for 1 millwatt output power. Put covers over attenuators. Remove glasses. Move optics package out of laser beam using the machine slide.
3. Place mask #1 and mask #2 as shown in diagram.
4. Using the adjustments on mirror mount #1 and mirror mount #2 point the laser beam through the center hole of each mask. The beam now is parallel to both the top and the edge of the table and in proper position.

5. Move the zoom lens so it is aligned with the laser beam. This alignment is usually not necessary. For details see separate alignment procedure.
6. Place mirror #3 between the zoom lens and mask #2. Adjust mirror #3 so the reflected beam passes through the center hole of mask #2 and then mask #1.
7. Remove mask #1.
8. NOTE: Do not adjust mirror mounts #1, #2, or #3 again.

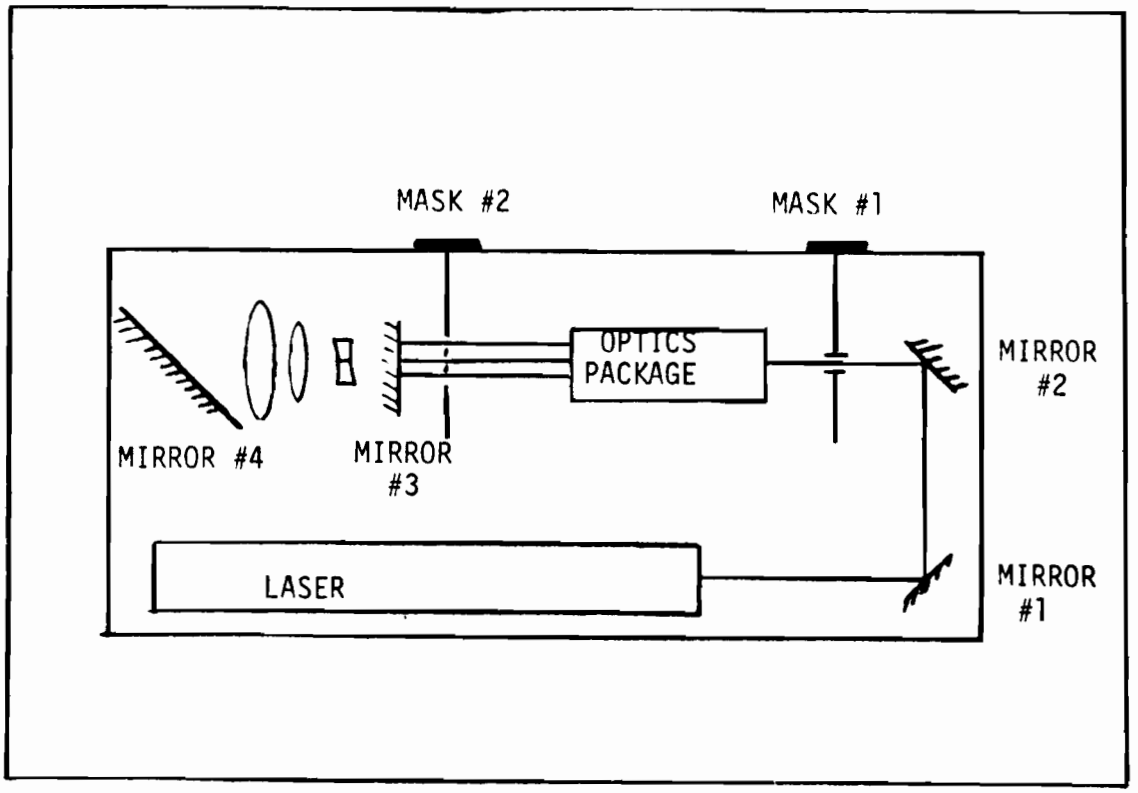

9. Move optics package into laser beam. The package should contain only the following sections: beam splitter, color splitter, the two photo tube sections and the lens mounting ring. (Note the beam waist adjuster and cover plate should not be attached at this time). Place alignment cover plate on optics package.
10. Adjust the jack screws and machine slide so the center hole of alignment cover plate is centered on the laser beam. (Rotating the optics package aids in establishing this criterion.)
11. Adjust the jack screws so the three output beams pass approximately through the center of the three holes in

the lens mounting ring section of the optics package.

12. Adjust the prisms (in the color splitter and beam splitter sections using an Allen wrench through access holes) of the three output beams to cause the beams to pass through the holes of the outer radius of mask #2 reflect off mirror #3 and back through mask #2. Note the optics package may have to be rotated to achieve this goal. It is generally not possible to obtain perfect alignment at this point.
13. Insert a hole alignment pin in the blue-green beam hole of the lens mounting ring section. Adjust the optical package jack screws so the blue-green beam passes through the small central hole.
14. Remove mask #2.
15. Insert hole alignment pins in the blue beam and green beam pins of the lens mounting ring section. Adjust their prisms so the beams pass through the small central hole.
16. Throughout steps 11-15, step #10 should be checked for any misalignment at the entrance of the optics package.

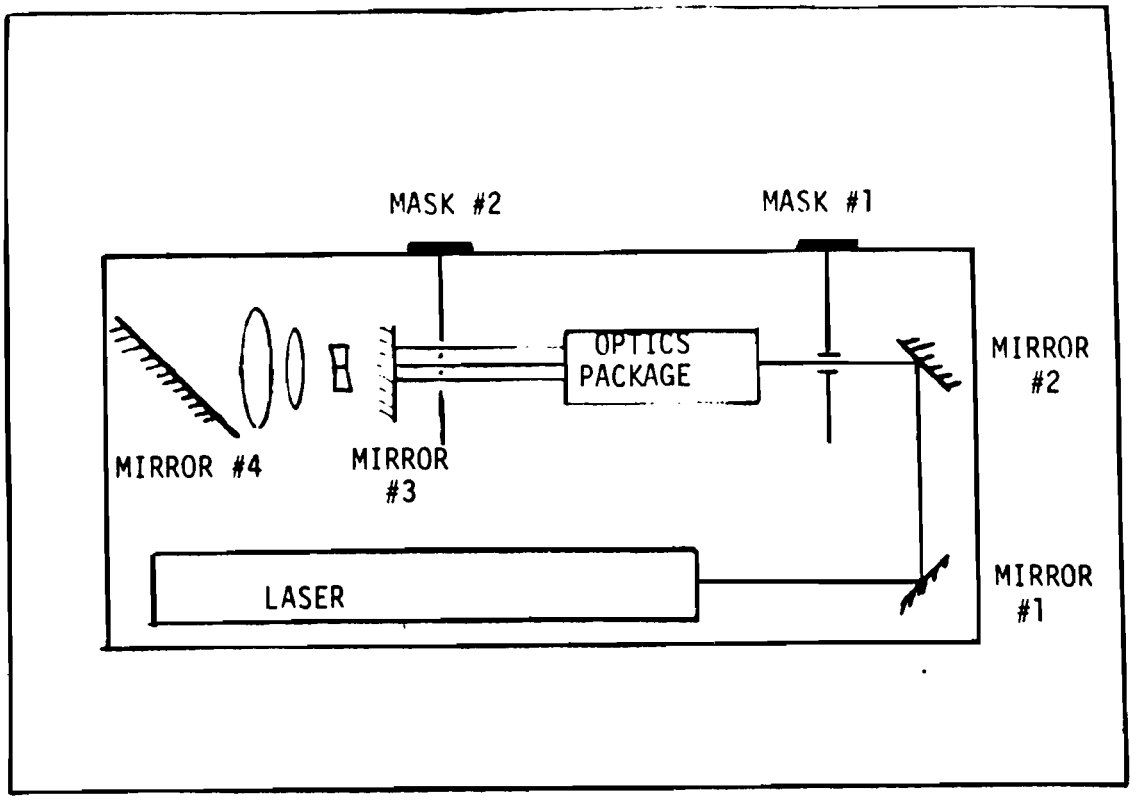

17. Remove the hole alignment pins. Attach the pinhole section to the optics package. Check that the three beams pass through the center of the output holes. There is no adjustment to be made.
18. Replace mask #2. Attach the beam translation section to the optics package. Adjust the prisms in the beam translation section (using an Allen wrench through the access holes) so that the three beams pass through the holes of the inner radius of mask #2, reflect off mirror #3 and back through mask #2.
19. Remove the alignment cover plate. Attach the cover plates and beam waist adjuster. Check that the beams are still aligned as in #18. Adjustments should not be necessary.
20. Remove mirror #3 and mask #2.

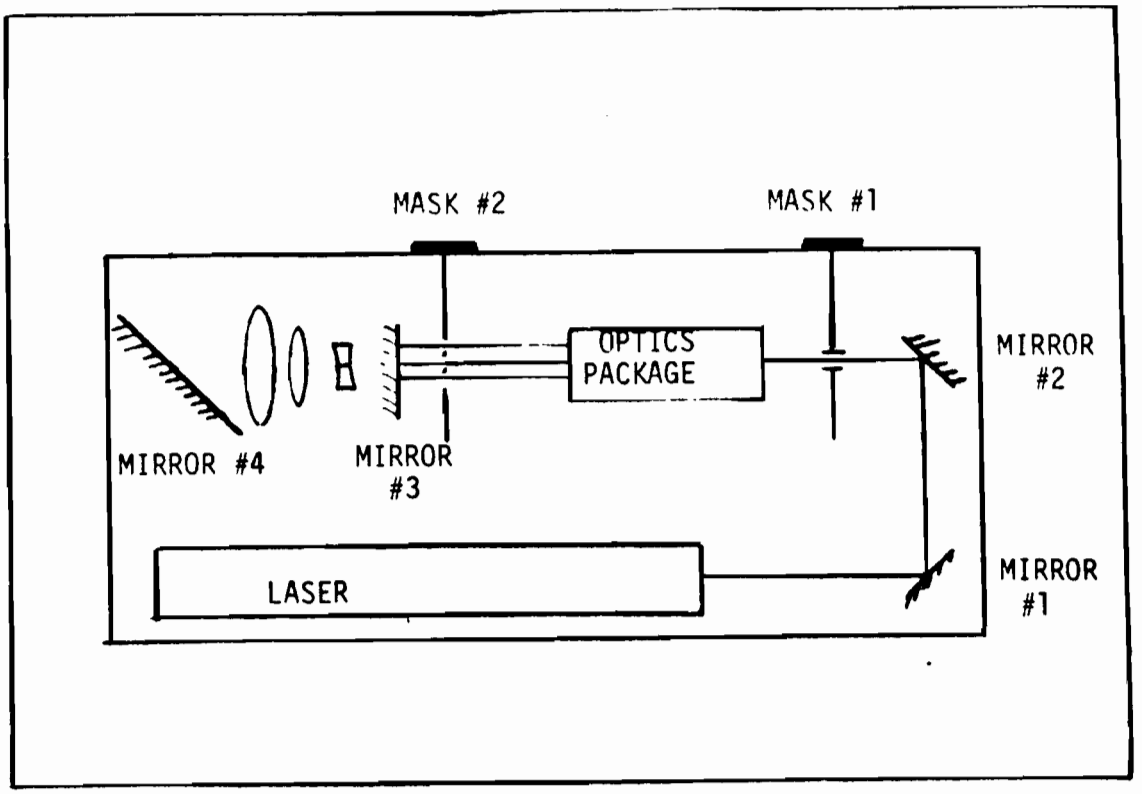

17. Remove the hole alignment pins. Attach the pinhole section to the optics package. Check that the three beams pass through the center of the output holes. There is no adjustment to be made.
18. Replace mask #2. Attach the beam translation section to the optics package. Adjust the prisms in the beam translation section (using an Allen wrench through the access holes) so that the three beams pass through the holes of the inner radius of mask #2, reflect off mirror #3 and back through mask #2.
19. Remove the alignment cover plate. Attach the cover plates and beam waist adjuster. Check that the beams are still

aligned as in #18. Adjustments should not be necessary.

20. Remove mirror #3 and mask #2.

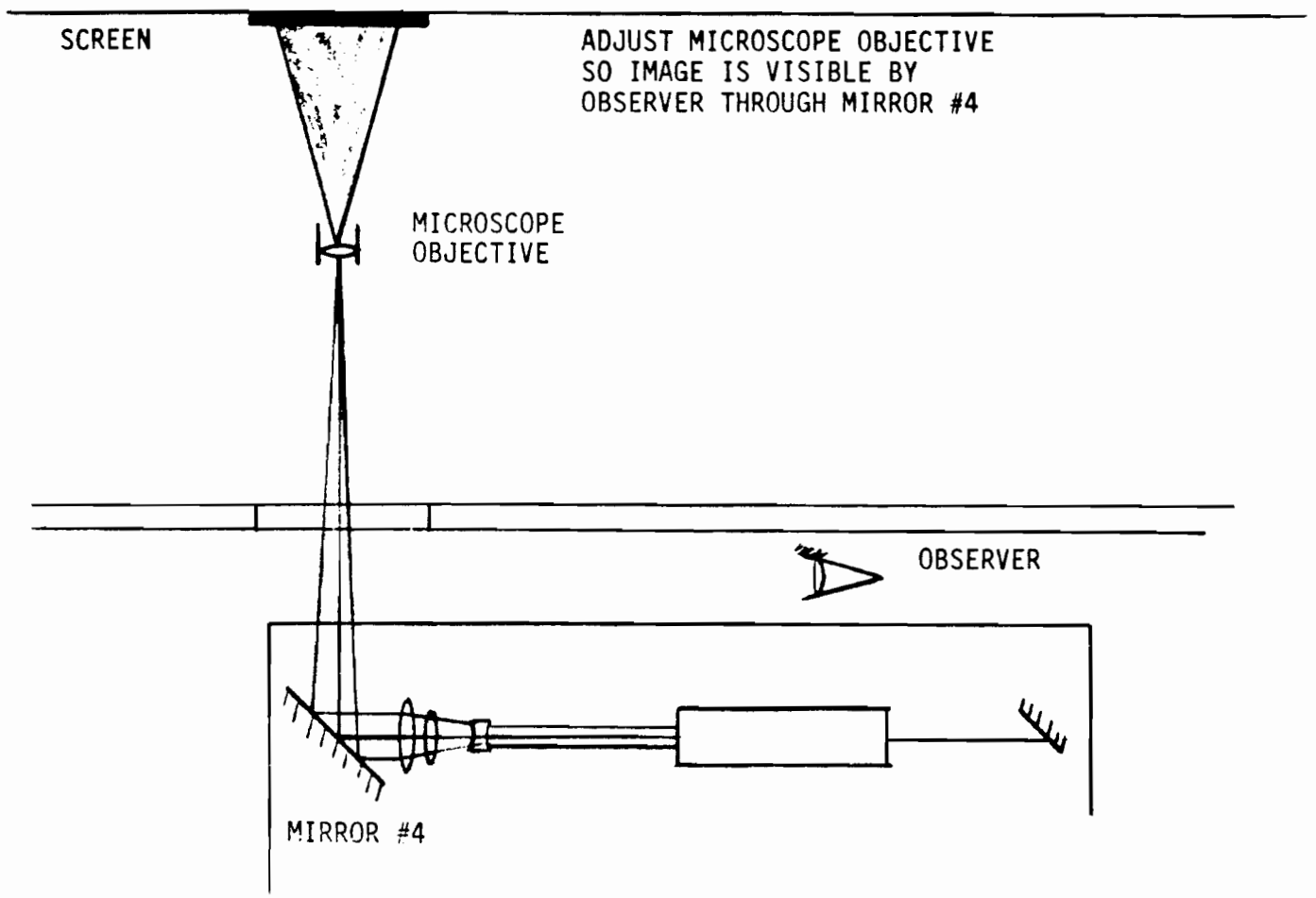

21. Place a microscope objective at the intersection of the three beams in the wind tunnel. Project the expanded beams onto a white screen. The three beams may not overlap completely at this point. Adjust the expanded beam image so it can be viewed from the optics package through mirror #4.
22. Adjust the beam waist adjuster so the projected beams have the minimum diameter.
23. Adjust the prisms of the beam translation section so the blue beam and green beam overlap the blue-green beam. This is the final adjustment of the transmission optics and is very sensitive and important for system

performance. After the first adjustment, zooming the zoom lens by hand so the projected beams are displayed before and after the crossover, aids in detecting any misalignment.

24. Set the zoom lens for best overlap. Looking through the 4880 Å filter repeat step #19 adjusting only the blue beam prism.

25. Set the zoom lens for best overlap of the blue beams. Looking through the 5145 Å filter adjust the green beam prism for maximum overlap of the green beams. Do not move the zoom lens during this adjustment.

26. Walk into the wind tunnel and check the blue and green fringes using their respective filters. The beam overlap should be excellent and fringes should have high contrast.

27. It may be necessary to repeat steps 23-26 several times to achieve optimum fringes.

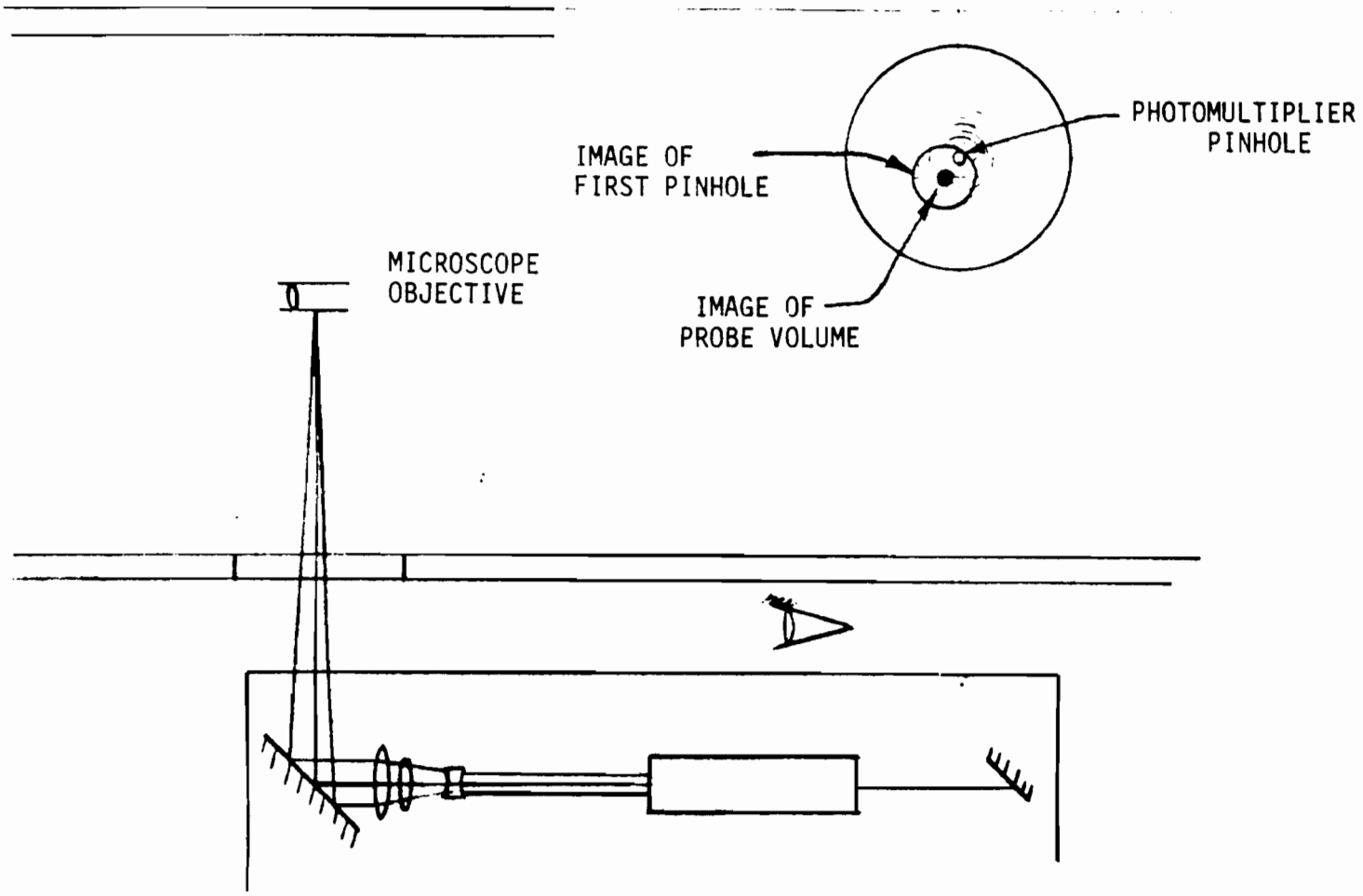

28. Place the microscope objective so that the beam crossing hits the side of the objective mount.
29. Look through the pinhole magnification lens of the blue phototube section. Adjust the pinhole in the pinhole section (using an Allen wrench through access holes) until an image of the crossover point is centered in an image of the pinhole of the pinhole section. Check that this condition is satisfied in the green phototube section.
30. Adjust the zoom lens by hand for minimum size of the overlap image as viewed through the blue phototube pinhole magnifier. While adjusting the zoom lens, sep-

arate images of all three beams can be seen. Set zoom lens so that these images overlap.

31. Adjust pinholes of the blue and then the green phototube sections so the image of the overlap regions focuses directly through the pinhole.

32. Remove the microscope objective.

33. It is possible that direct specular reflections off the zoom lens may be entering the phototubes through the pinholes. There should be no laser light at the pinholes with nothing in the probe volume. If reflections are observed, very slight movement of the zoom lens is necessary to remove them.

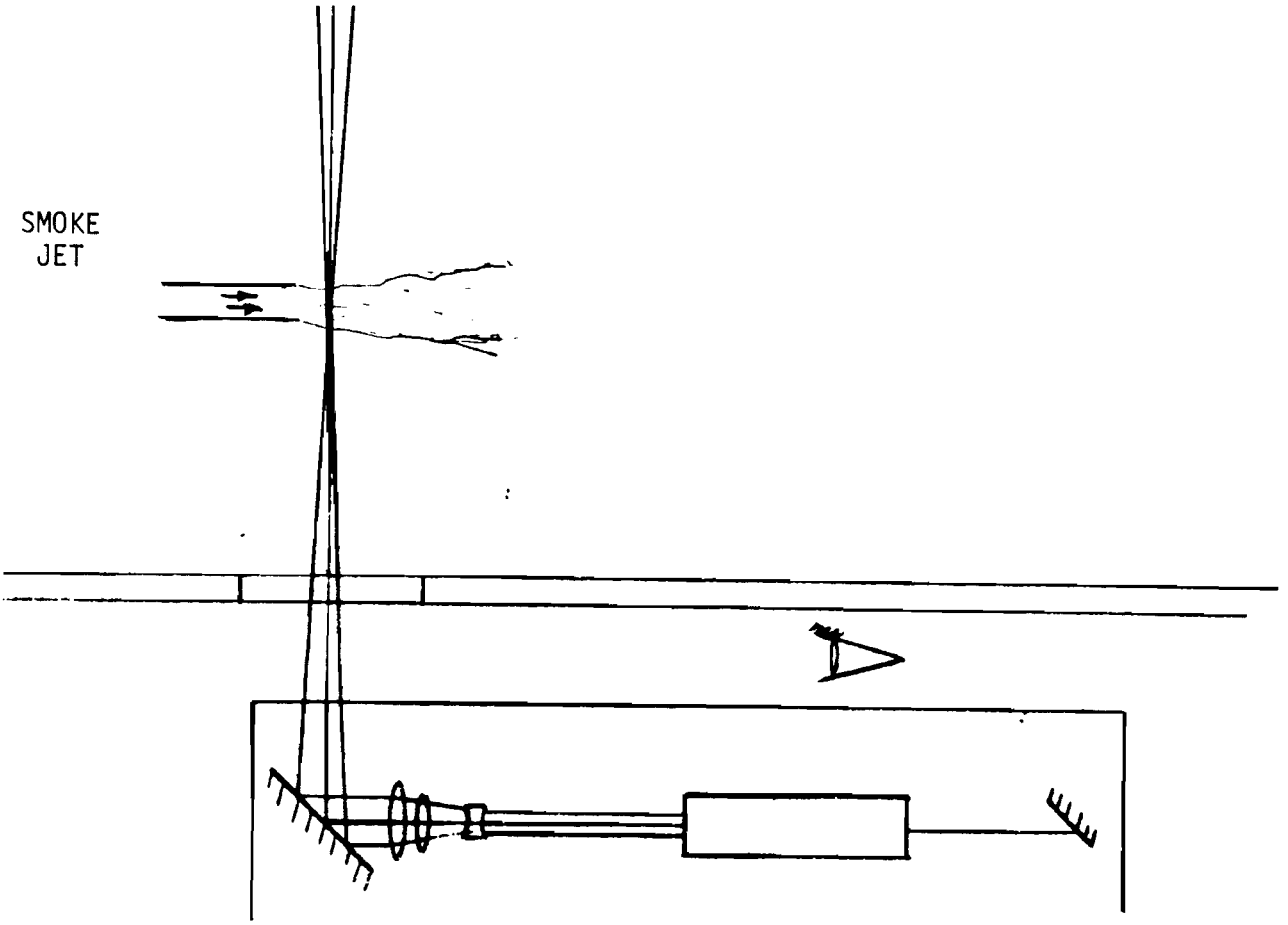

34. Place the smoke jet, so that there is a flow through the probe volume.
35. Turn on phototubes. Adjust voltage for 2,000 volts.
36. With safety glasses on, remove the attenuators and set laser power to 1.0 watts.
37. Look at the output of the phototubes on an oscilloscope. Make sure that the cables are terminated with a 50Ω load. The output should contain doppler frequency bursts comparable to the examples provided. The output can be "peaked up" by adjusting the blue and green pinholes while viewing the oscilloscope.

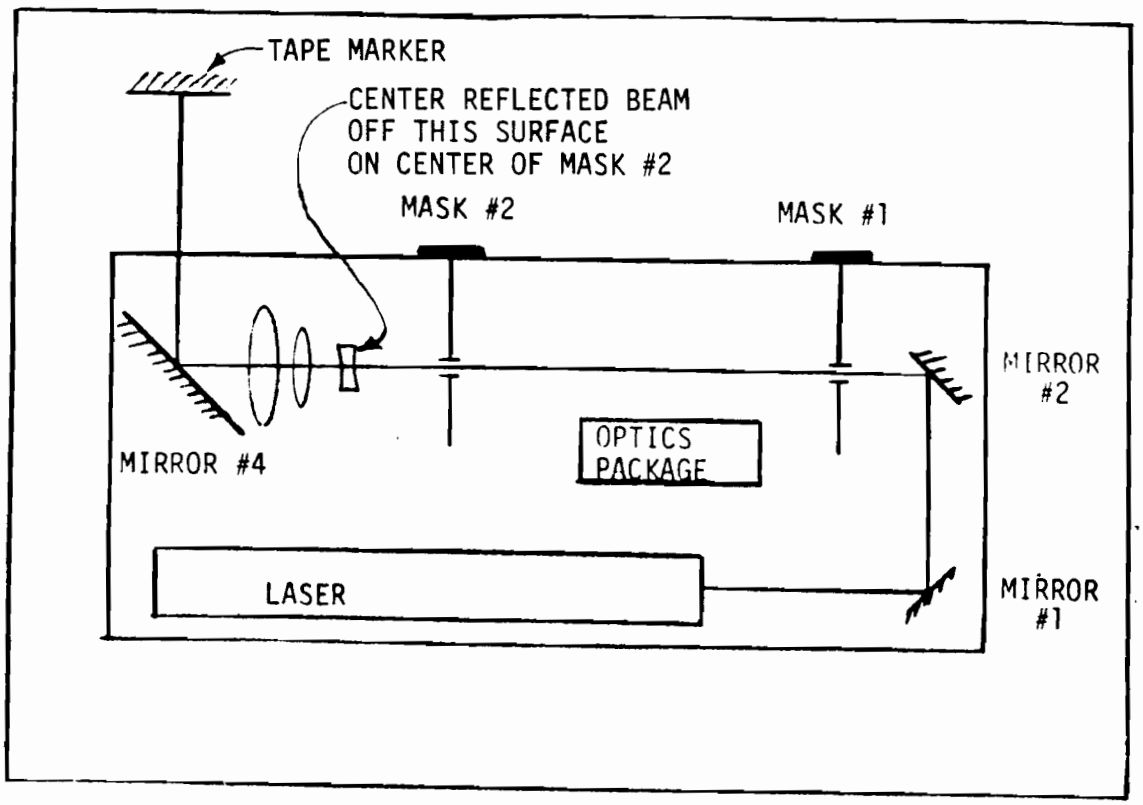

ZOOM LENS ALIGNMENT

1. Move zoom lens out of laser beam path.
2. Use mirror #1 and mirror #2 to point the beam through the masks #1&2.
3. The beam will reflect off mirror #4 and hit the wind tunnel. Mark this spot with a piece of tape with a cross on it.
4. Move the zoom lens into the beam path.
5. Position the zoom lens so the output beam is centered on the cross on the tape and the reflected beam from the first element of the lens is centered in the hole of mask #2.

SIGNAL PROCESSING

METHODS OF MEASURING THE FREQUENCY (f_D)

SPECTRUM ANALYZER

COUNTERS

TRACKERS

A/D CONVERTERS / FFT

PHOTON CORRELATOR

Original Signal

Threshold (After HPF)

a) Output of Schmitt

b) N/2 Cycle Time ($\tau_{N/2}$)

c) N Cycle Time (τ_N)

d) Total Burst time (τ_B)

Output Update (If $\left| 1 - \frac{2\,\tau_{N/2}}{\tau_N} \right| \leq \Delta$)

Data Ready Signal

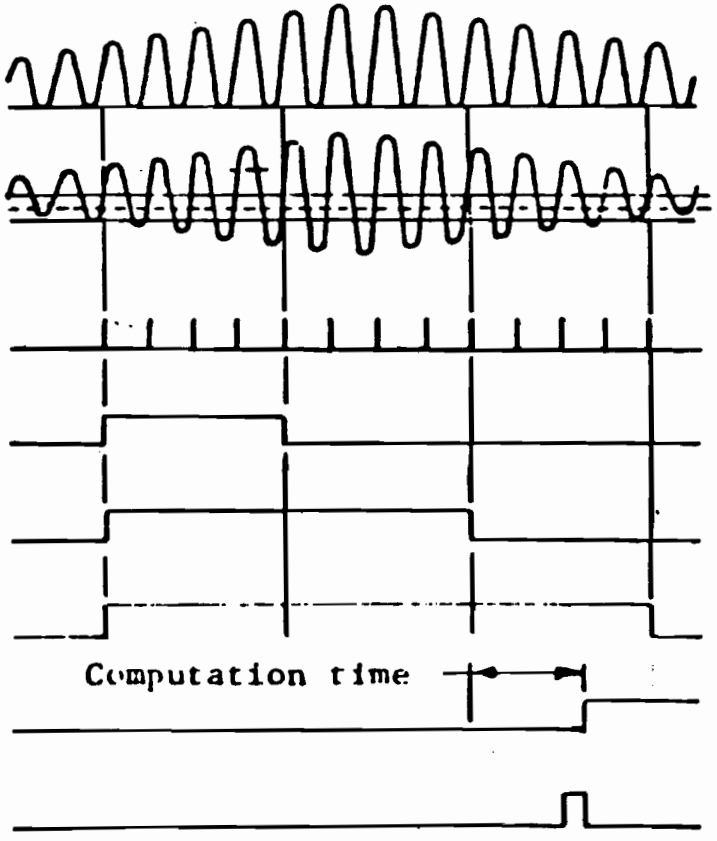

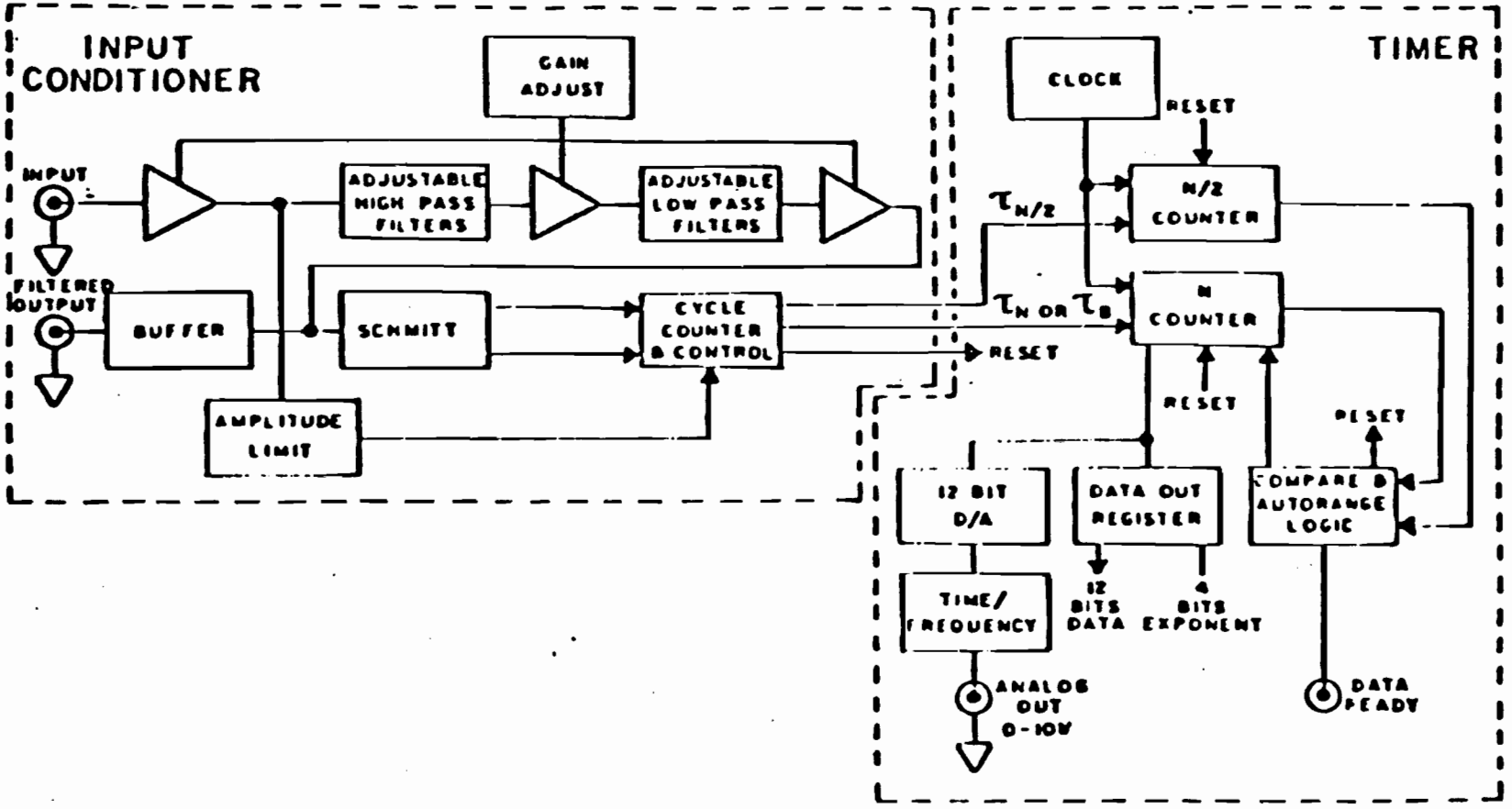
INPUT CONDITIONER
GAIN ADJUST
INPUT
ADJUSTABLE HIGH PASS FILTERS
ADJUSTABLE LOW PASS FILTERS
FILTERED OUTPUT
BUFFER
SCHMITT
CYCLE COUNTER & CONTROL
RESET
AMPLITUDE LIMIT
TIMER
CLOCK
RESET
N/2 COUNTER
$\tau_{N/2}$
τ_N OR τ_B
N COUNTER
RESET
RESET
12 BIT D/A
DATA OUT REGISTER
COMPARE & AUTORANGE LOGIC
TIME/ FREQUENCY
12 BITS DATA
4 BITS EXPONENT
ANALOG OUT 0-10V
DATA READY

DATA PROCESSING

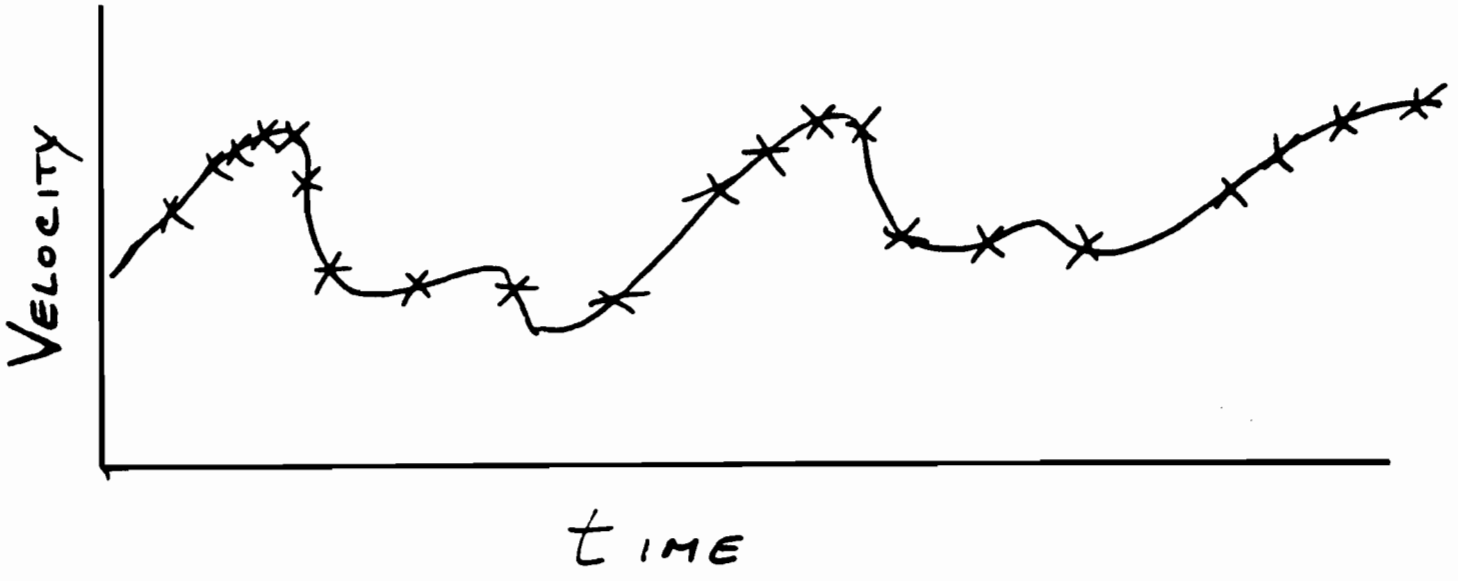

- TIME BETWEEN DATAPOINTS IS RANDOM
- MORE DATA POINTS AT THE HIGHER VELOCITIES
- CAN LEAD TO BIASING OF STATISTICS

Example

Square Wave Velocity

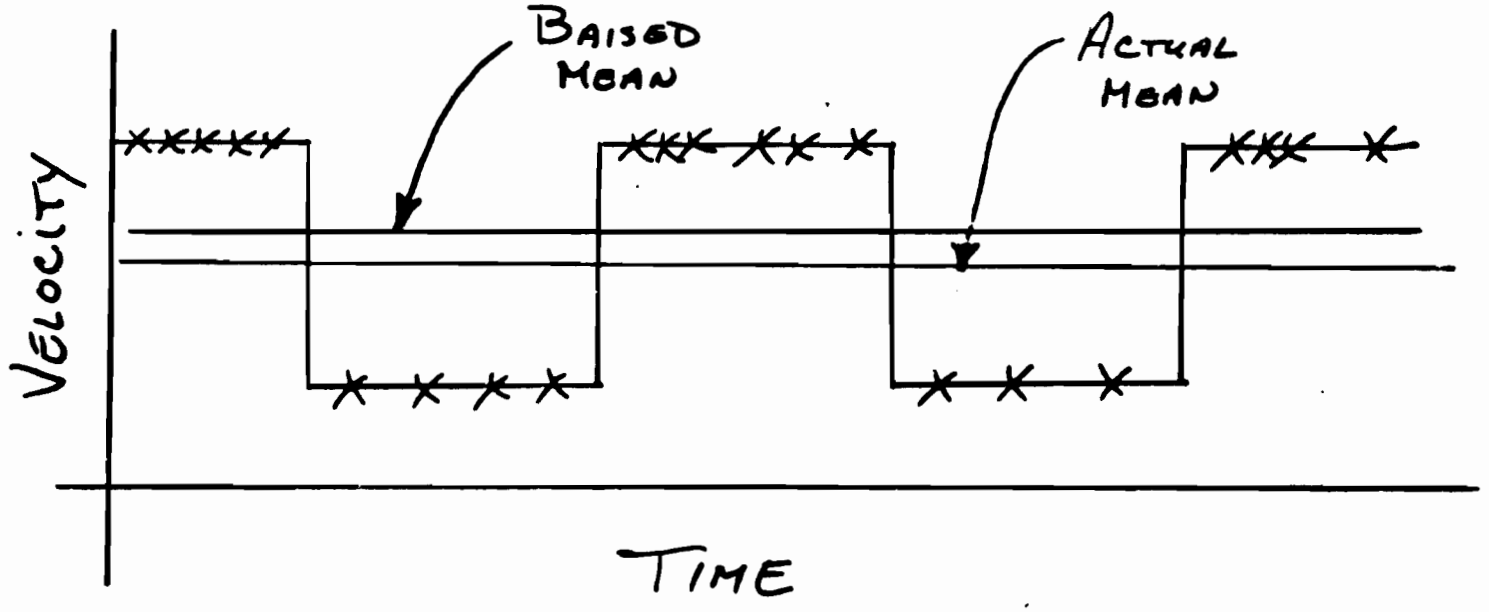

Baised Mean Velocity

$$\overline{u} = \frac{\sum_i u_i}{N}$$

;ignal Processing

e photodetector output is a frequency that varies with particle iocity. To convert this to a voltage or "number" proportional to locity requires some type of frequency converter. The ermittency of the signal, noise, variable amplitude and high quencies require sophisticated electronics to properly convert ; frequency to a voltage or number that is more directly useable.

ıfortunately, there is no universally optimum technique. ectrum analyzers were used first, with frequency trackers, oton correlators and burst counters following. Another chnique is to go directly to a computer with a fast A/D converter the photodetector signal [H]. Details of the TSI tracker and unters can be found in the Signal Processors Section of this talog. In the following some general comments are made ıch will assist you in making the correct selection.

ow Photon Density

ıth low photon density signals (low light flux) a measure of ıriations in the photon rate is required to analyze the signal. ypically, a photon correlator has been used for this purpose.

ıe photon correlator is fundamentally very similar to an analog ırrelator used in the auto-correlation mode. The primary fferences are as follows:

1) Correlations are made on a photon count instead of an analog voltage level.

2) The speeds required (minimum $\Delta\tau$) are generally higher for photon correlation.

3) A high product rate is more important for photon correlation.

Item (2) is present because many of the difficult LDV measurements involve signal frequencies over 10 MHz. Item (3) is relevant because data is often present only intermittently so it is important to use the available signal efficiently.

An alternate signal processor when only low frequencies are involved (e.g. free convection) is a Fast Fourier Transform (FFT). These use the data efficiently with the multi-bit multipliers and give a readout in frequency rather than time. However, they are only useful up to a Doppler frequency of about 100 KHz.

The primary disadvantage of either the photon correlator or the FFT is that at present only average data is available. In other words, the output is very similar to taking an analog auto-correlation or spectrum of an analog signal from the photodetector at high photon density. The mean value of the velocity is measured easily (and correctly) with a measure of the turbulence intensity also available after some computation. More details are available only by significantly speeding up the time to make a correlation — at which point concerns about the relation between photon rate and data biasing must be addressed.

The primary plus of photon correlation is that it will make measurements under conditions that are beyond the capabilities of other processors. For example, low photon density may be unavoidable because of limitations on laser power and/or the need to backscatter long distances.

Data Density

Previously, we have introduced the concepts of photon density and burst density. In the case of high photon density and low burst density, it is convenient to introduce the concept of data density. As defined here, data density refers to the time between successive, measurable signal bursts compared with the time scale of the velocity fluctuations. Specifically it is equal to the data rate [N = no. samples/second] times the Taylor microscale of the signal T.

Figure 16 illustrates the concept of data density in terms of the output of a signal processor that can make discrete measurements on individual Doppler bursts. The continuous trace indicates the actual velocity signal while the dots indicate measurements on Doppler bursts by a signal processor. The top

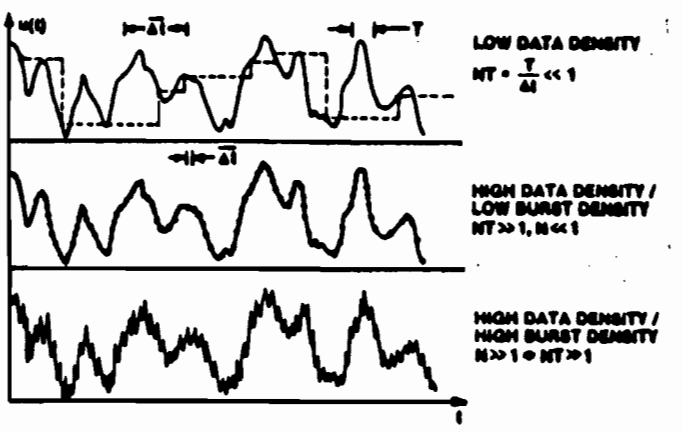

FIGURE 16. Types of Signals

trace represents low data density while the center trace represents high data density. The bottom trace is the high burst density case (also, of course, high data density) where phase noise is shown added to the velocity signal. Since most signal processors hold the last reading when no new data is present, the dashed line on the top trace represents the output of a signal processor.

The data density is an important concept because it can affect both the optimum choice of signal processor and the required data analysis procedures. It should be emphasized that correlators or spectrum analyzers that average are not significantly affected by either data density or burst density, except for the required averaging time. However, if one could get the correlation or spectrum of single bursts, then similar concepts would apply to these instruments — even including the low photon density case.

Tracker Type Processor

A tracker type processor uses a bandpass filter and frequency discriminator to "track" the frequency changes in the photodetector output. The use of the bandpass filter permits a tracker to operate on Doppler signals that have a relatively poor signal-to-noise ratio. It is perhaps most frequently used on high burst density signals, although it will operate satisfactorily on most low burst density signals if the data density is high (trace two, Figure 16). The output of most trackers is an analog voltage proportional to the input frequency.

The most significant limitation of tracker type processors is in the low data density case (trace one, Figure 16). Through a feedback circuit, the input Doppler frequency for a tracker is mixed to fall into the range of the bandpass filter. However, in the low data density case, the next Doppler burst may have a frequency that lies outside the filter bandwidth. In this case no signal gets through to adjust the feedback circuit and the data is lost. This, of course, is not acceptable. Increasing the bandwidth of the bandpass filter can reduce this problem, but this also reduces the ability of the tracker to extract the signal from the noise. On the other side, with high burst density signals, making the bandwidth narrow to eliminate noise will limit the ability of the tracker to "track" rapidly. In addition, with narrow filter bandwidths, the tracker can mistake random noise for a Doppler signal.

Tracker type processors are normally quite easy to use. They provide an analog output and can have a wide dynamic range as well as the ability to follow quite rapid fluctuations in the flow. They will work well in almost all high data density applications. At low data density, the range of frequency changes between successive Doppler bursts must be within the filter bandwidth (capture range) of the tracker to guarantee reliable measurements.

Counter Type Processor

The counter type signal processor will operate at any burst density or data density as long as the signal-to-noise ratio is adequate. However, it is most often associated with low data density since it overcomes the limitation of tracker type processors in this application.

The counter basically measures the time, τ_i for n_i cycles of the Doppler signal. The frequency is then calculated from $f_{D_i} = n_i/\tau_i$. Since the time τ_i, is generally measured with a digital clock, the fundamental output of a counter is a digital word proportional to the time for n_i cycles. The value of n_i may either be fixed or variable and output as another digital word.

On a counter, input filters are provided and set to filter out the "pedestal" and as much of the noise as possible without restricting the Doppler signal. When very wide dynamic ranges are encountered, it is often necessary to use frequency shifting to permit effective filtering of the pedestal component. This is particularly true when the optics gives relatively few fringes (cycles) in the measuring volume.

In summary, the counter requires a somewhat higher signal-to-noise ratio than the tracker but will operate over all ranges of burst density and data density. The fundamental output is digital and computer data reduction is often used — particularly since the low data density case requires special data reduction procedures. This is described in more detail in the next section.

Data Processing

Once the signal processor has converted the signal from a frequency to a voltage (or number) proportional to velocity, the next step is to analyze the data for the required information. The data analysis procedure depends on the signal processor used as well as the burst density and data density.

In addition to mean velocity, fluctuation statistics are often of interest. These include:

Amplitude Information (rms, Reynold stress, higher order moments, amplitude probability distribution)

Temporal Information (correlation with time delay, power spectrum)

Spatial Information (two point spatial correlation)

Conditional Averages

Wave Form

At high photon density all of this data can be extracted from laser velocimeter data. Even at low data density, in theory it is only the last item — particularly in terms of actual transient waveform — that cannot be obtained from LDV data.

In the following, data processing procedures for averaging type processors will not be covered and the reader is referred to the literature [D, I]. Instead, the assumption is made that accurate measurements are made on individual data bursts.

High Data Density

In the high data density case, it is often sufficient to simply use the analog output of a tracker or counter and standard data handling instruments such as a time average for mean flow, an rms meter, an amplitude probability analyzer, an analog correlator or spectrum analyzer, or an oscilloscope (to view the transient waveform). In this case, a low pass filter is set at the minimum position that will still allow the frequencies of interest to pass while filtering the steps caused by the "sample and hold" aspects of the signal processor output (Figure 16).

In some cases, particularly with counter type processors, it may be desirable to go directly to computer data reduction even in the high data rate case. It is then best to use the trapezoidal rule to correct for the fact the data is not naturally divided into equal time increments. If the trapezoidal rule is not convenient, sampling the low pass filtered signal at uniform time increments is often adequate.

It should be emphasized that even in the high data rate case, using the data points as they are measured may not give the right answer. When large fluctuations are present, one must use time as the base for taking data — or use something like the trapezoidal rule to essentially correct to a time base. In some cases, even when the data density is quite high, the procedures of the next section may be used to extract more information from the data.

Low Data Density

In the low data density case, often insufficient data points are obtained to even recognize the underlying transient waveform on an oscilloscope. Then the correct mean value cannot be obtained by either a time average or a data average. This problem arises because more particles will go through the measuring volume per unit of time at high velocity than at low velocity. This will distort both a data average or a time average toward the high velocities.

The simplest correction to this problem for mean velocity is to only average the data while the measurement is being taken. For example, on a tracker one would only use the data while the tracker was actually locked onto a signal from a particle in the measuring volume. Although this would work with trackers, counters give a new output only after some computations are made rather than during the measurement. As explained previously, counters are applicable to a wider range of flows when the data density is low. Therefore, the following discussion is directed at counter type processors.

With a counter, the time across the measuring volume is the time, τ_{Bi} for the total number of measurable Doppler cycles, n_i across the measuring volume. This data can then be used to weight the output properly as well as give the particle velocity.

For example, for mean velocity:

$$\bar{u} = \frac{\Sigma u_i \tau_{Bi}}{\Sigma \tau_{Bi}}$$

This can be further reduced since:

$$u_i = \frac{n_i}{\tau_{Bi}}$$

$$\text{then: } \bar{u} = \frac{\Sigma n_i}{\Sigma \tau_{Bi}}$$

Similar procedures are used for other data. For the amplitude probability distribution one would:

1) Measure u_i from n_i and τ_{Bi}
2) Measure transit time, τ_{Bi}
3) Input a number proportional to transit time, τ_{Bi}, into the correct velocity increment.

From the amplitude probability analysis the mean, rms, and higher moments can all be calculated.

To get frequency data, the random arrival of particles (data points) can actually be used to advantage to extend the spectrum beyond that expected when considering the average data rate. Again, appropriate weighting by τ_{Bi} is required. The result of this reasoning can be expressed in the following equation for the auto correlation:

$$C_{uu}(n\Delta\tau) = \frac{\sum_{i<j} u(t_i)\,\tau_{Bi}\,u(t_j)\,\tau_{Bj}}{\sum_{i<j} \tau_{Bi}\,\tau_{Bj}}$$

when:

$$(n - 1/2)\Delta\tau \le t_j - t_i < (n + 1/2)\Delta\tau$$

where:

τ_{Bi} = total burst time for velocity point $u(t_i)$
τ_{Bj} = total burst time for velocity point $u(t_j)$
$\Delta\tau$ = time delay interval
t_i, t_j = times at which ith and jth data points occurred.

Computer Data Analysis

From the previous discussion, it becomes evident that, particularly at low data density, data analysis with a computer is recommended and in some cases a requirement. Figure 17 shows a recommended system using a direct memory access (DMA) to a computer. Most minicomputers have these interfaces available and permit up to 500,000 16 bit words per second to be transferred to memory. This is sufficiently fast for LDV and avoids the need of any type of separate buffer. If more data is to be taken than can be stored in the computer memory, the data can subsequently be transferred from the computer memory to some type of mass storage such as a tape or disc. Details of TSI hardware for interfacing one or more counter type processors to a computer through DMA are discussed in this catalog.

The above implies a dedicated computer located within a few meters of the signal processor. An alternate is to go directly to a

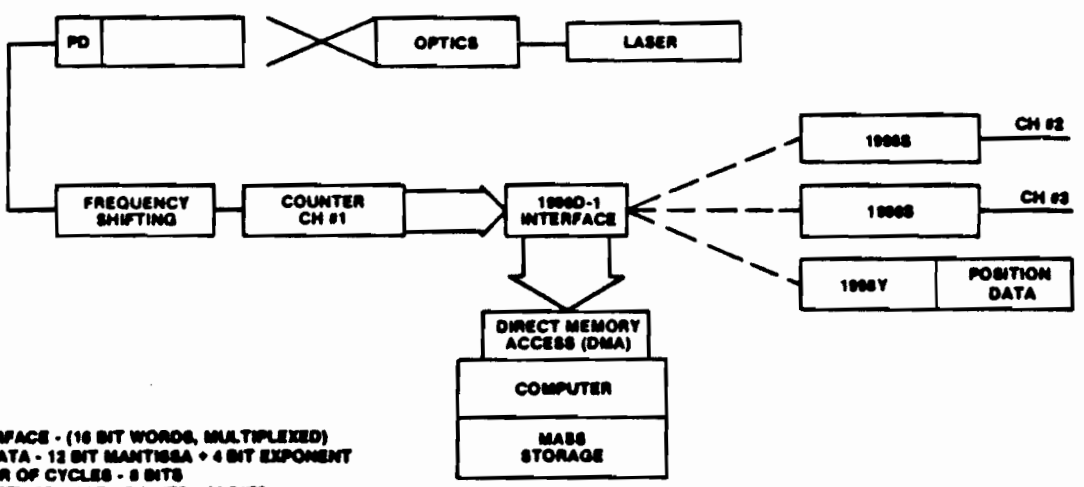

FIGURE 17. Typical Data Acquisition System — Counter